Drew University

College of Liberal Arts

Impacts of Pine- and Lemon-Based Cleaners on Indoor Air Quality

A Thesis in Chemistry

By

Virginia Gaylord

Submitted in Partial Fulfillment

Of the Requirements

For the Degree of

Bachelor of Science

With Specialized Honors in Chemistry

December 2022

Acknowledgements

I would first like to thank my research advisor, Dr. Hinrichs. I have learned so much from him have thoroughly enjoyed working in his lab. Without his guidance and support, this project would not have been possible. I would also like to thank my committee members. Dr. Pearsall encouraged me to pursue a chemistry major even though I wasn't sure I could, and for that I'm so grateful. Dr. Dunaway has also been incredibly encouraging and always challenged me to think one step further. I also owe thanks to Hannah Primiano, a fellow member of Dr. Hinrichs' research group. Hannah introduced me to the lab and was always willing to help me out. I thoroughly enjoyed all the hours we spent in lab together and could not have asked for a better lab partner. I would also like to thank my parents, friends, teammates, and coaches, all of whom have been cheering me on since the beginning of this project; I truly could not have done this without them. Lastly, I want to thank the Drew University Chemistry Department. I have had such an amazing experience at Drew, and every faculty member has been extremely supportive throughout this process. Thank you all.

Abstract

Common household cleaning products contain organic compounds, such as terpenes, that react with ozone to produce volatile organic compounds (VOCs). VOCs often have negative effects on indoor air quality. This study investigated VOCs formed from reactions of two commercially available cleaners containing terpenes (a pine-based cleaner and a lemon-based cleaner) with ozone to determine how these reactions affect indoor air quality in both the gas and thin film phases. To monitor gaseous products of reactions between ozone (in the gaseous state) and multi-phase VOCs, a laminar flow reactor was coated in each of these cleaners and exposed to ozone via an ultraviolet lamp connected to the reactor, with a Fourier transform infrared spectrophotometer (FTIR) continuously monitoring the reactions and an ozone monitor continuously recording ozone concentrations. IR spectra revealed that the pine-based cleaner and ozone reaction yielded several VOCs containing hydrocarbon, carbonyl, and alcohol functional groups. The VOCs from this reaction differed over the course of the reaction, with at least two distinct products observed, one of which is 2,2,4-Trimethyl-3-oxovaleraldehyde. The IR spectra from the reaction of the lemon-based cleaner with ozone showed VOCs containing hydrocarbon and carbonyl functional groups that matched the original spectrum of the lemon-based cleaner without ozone. This reaction did not result in a new product, but the presence of ozone enhanced the release of compounds already present. The reactive uptake coefficient for ozone loss on the pine-based cleaner (calculated from ozone concentrations during each reaction) was approximately 1.4 x 10^{-5} upon first exposure to the cleaner and 4.5 to 5.62 x 10^{-6} after 40 minutes of exposure and did not change at different relative humidity levels. For the lemon-based cleaner, the initial reactive uptake coefficient of ozone was approximately 1.25 to 1.48 x 10^{-5} upon and 6 to 6.25 x 10^{-6} after 40 minutes of exposure. No significant difference was observed in reactivity with ozone between the lemon- and pine-based cleaners. These results show that use of terpene-containing cleaning products leads to VOC production and thus negatively impacts indoor air quality.

Table of Contents

Chapter 1: Introduction

1.1: Indoor Air and Pollutants

In most developed countries, the average person spends approximately 90% of their day indoors (Fu et al., 2013). Indoor chemistry is thus an important field of study to determine the quality of indoor air and its effects on human health. Although indoor chemistry is heavily influenced by the respective outdoor environment, the enclosed environment often results in higher concentrations of pollutants indoors as compared to outdoors, which can be particularly disastrous for human health (Weschler, 2011). In the indoor environment, concentrations of organic compounds tend to be higher than in the outdoor environment (Weschler and Carslaw, 2018). Additionally, indoor environments have more surfaces than outdoor environments upon which chemical reactions can occur (Abbatt and Wange, 2020).

Many pollutants are known to have negative effects on human health and thus have maximum recommended concentrations to which a person should be exposed. Gaseous ozone is one such pollutant. Indoor ozone concentrations are heavily influenced by the concentrations of ozone in the outdoor environment. The World Health Organization (WHO) publishes recommendations for maximum pollutant exposure in the indoor environment. Ozone is recommended to exist at no greater than 50 ppb in the indoor environment for a period of eight hours (Nazaroff et al., 2022). Long term exposure to concentrations of ozone greater than 50 ppb can cause negative health effects, most notably respiratory diseases (World Health Organization). Particulate matter is also a common indoor pollutant known to cause negative health effects. Different types of particulate matter are defined by size, and smaller classes of particulate matter are known to enter the respiratory and cardiovascular systems, contributing to diseases of these systems (World Health Organization). Maximum recommended exposure to particulate matter varies based on the size. The World Health Organization recommends maximum average exposure to $PM_{2.5}$, or fine particulate matter (diameter smaller than 2.5 µm), of $5\mu g/m^3$, and an average exposure to PM_{10}, or coarse particulate matter (diameter smaller than 10 μm) of 15 $5\mu g/m^3$. Erickson et al. identified $PM_{2.5}$ as the pollutant most dangerous to human health in the present day (Erickson et al., 2020). Nitrogen dioxide and sulfur dioxide are two other gaseous pollutants with WHO- recommended maximum exposures due to their negative health effects, which are 19 ppm and 105 ppm, respectively (World Health Organization). Unfortunately, in 99% of the world, such pollutants exist in the outdoor environment at much higher levels than these standard values, which heavily impacts how these pollutants penetrate the indoor environment (World Health Organization). Thus, understanding how these pollutants are formed in and/or penetrate into the indoor environment is essential in improving indoor air quality.

1.2: Indoor Ozone

As ozone is a prevalent pollutant in the indoor environment, its concentrations serve as an important determinant of indoor air quality. Ozone is a pollutant with many negative health effects, which can include respiratory distress and even DNA damage (Wisthaler et al., 2005; Salonen et al., 2018). Although the World Health Organization recommends 50 ppb as the maximum safe concentration of ozone in indoor environments, negative health effects have been observed at lower concentrations (Salonen et al., 2018).

The most dominant source of ozone in the indoor environment is leakage from the outdoor environment. At the ground level, ozone is generated outdoors through the photochemical reaction of nitrogen oxides (including nitrogen dioxide) with ultraviolet light, as shown below (Erickson et al., 2020).

$$(1)\ NO_2 + hv \rightarrow NO + O$$

$$(2)\ O + O_2 \rightarrow O_3$$

Urban environments tend to have higher ozone concentrations than rural and suburban environments due to increased pollution from nitrogen oxides (Zhong et al., 2016; Weschler and Carslaw, 2018). Such reactions cannot occur indoors due to the absence of direct ultraviolet light from the sun. Environments which lack sunlight will have lower concentrations of ozone as well. HVAC systems can also affect the circulation of air in the indoor environment, which can alter the products and rates of indoor chemical reactions. In a typical indoor environment, the ozone concentration is approximately 20 to 70 percent of the corresponding outdoor environment as outdoor ozone permeates the indoor environment through the opening of windows and doors (Chen, 2010). Therefore, variance in the concentration of ozone in the outdoor environment based on environment and/or season will have a direct impact on indoor ozone levels.

Indoor appliances can also affect indoor ozone concentrations. Appliances such as photocopiers, air purifiers, and printers can produce ozone and vastly increase the indoor ozone concentration (Weschler et al., 2018; Salonen et al., 2018). When in use, these appliances produce ions and electrons (Tipayarom and Tipayarom, 2011). Such ions and electrons then react with oxygen gas produced by the appliance (from electrophotography and the corona wire) to form ozone (Tipayarom and Tipayarom, 2011). However, the harmful effects of such appliances were determined fairly recently; air purifiers known to produce ozone were advertised as more efficient air cleaners and sold until the early 2000s, when regulatory agencies identified these products as harmful to human health (Weschler, 2000). Since ozone is now a well-known pollutant, studies have determined that environments in which ozone-producing appliances are frequently used, such as office buildings, can thus have elevated ozone concentrations, which can have negative health effects on occupants.

Along with being an indoor pollutant, ozone is also extremely reactive in the indoor environment. While the amount of ozone is lower indoors as compared to outdoors, indoor ozonolysis products tend to be more volatile than outdoor ozonolysis products due to the high usage of terpene-containing products in the indoor environment (Goldstein et al., 2020; Milhelm et al., 2020). Additionally, the specific concentration of ozone is not necessarily significant in its reactivity nor its overall effect on indoor air quality; Liu et al. observed VOC formation in an indoor environment at an ozone concentration of only 4.3 ppb (Liu et al., 2021). Indoor ozonolysis can also produce secondary organic aerosols (SOA), a subclass of fine particulate matter that contains volatile compounds and is known to have negative effects on human health (Donahue et al., 2007). The presence of ozone in the indoor environment poses a major problem when considering how to improve indoor air quality; while some studies recommend increased ventilation when VOC-containing products are used, this can lead to an increased quantity of ozone molecules with which VOCs can react (Singer et al., 2006; Salonen et al., 2018). Due to the presence of ozone in the indoor environment, reactions of ozone with household VOC-containing cleaning products are commonly conducted to understand how indoor air quality is affected by such reactions.

1.3: Sources of Volatile Organic Compounds (VOCs): Indoor Cleaning Products

Indoor cleaning products are a significant source of reactive trace gases in indoor air. Such cleaning products often contain volatile organic compounds (VOCs), which are defined as organic compounds with high vapor pressures and low boiling points. VOCs are known to have negative effects on human health (Chiu et al., 2009). The impacts of VOCs on human health can range from mild irritation to disease and illness, including of the respiratory, endocrine, and central nervous systems (Chiu et al., 2009). Certain VOCs such as benzene and formaldehyde are carcinogens (Chiu et al., 2009; Huang et al., 2012). Within VOC-classified compounds, the level of volatility can widely vary (Singer et al., 2006). The volatility of a compound is partially dependent on its molecular weight; while higher volatility compounds, such as formaldehyde, have relatively small molecular weights, larger VOCs tend to be less volatile (D'Ambro et al., 2017). This is consistent with the properties of VOCs; larger VOCs will have higher boiling points due to stronger intermolecular forces present in the molecule and thus will be less volatile. For instance, formaldehyde has only dipole-dipole and London dispersion forces, which are relatively weak. In contrast, higher molecular weight compounds will have stronger intermolecular forces (ie, hydrogen bonding) and thus will have greater boiling points and be comparatively less volatile.

Many indoor cleaning products VOCs contain terpenes (Weschler and Carslaw, 2018). Terpenes are a class of volatile aromatic compounds with the general formula $(C_5H_8)_n$, where n can vary. Commonly observed terpenes include D-Limonene, α-Terpineol, and γ-Terpinene, all of which are shown in Figure 1.

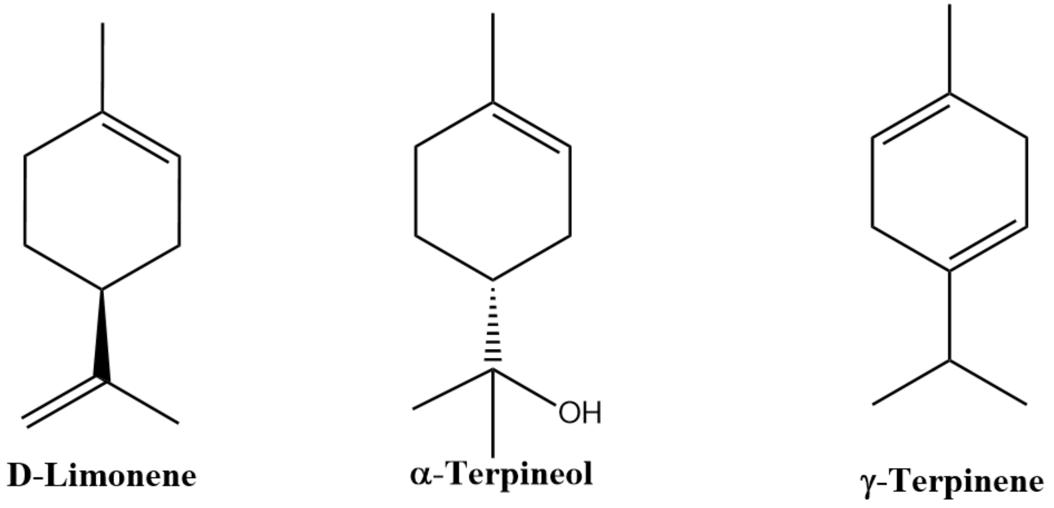

Figure 1: Terpenes Commonly Present in Cleaning Products.

Terpenes undergo ozonolysis quickly due to their alkene group (Huang et al., 2012). While terpenes in general are highly volatile, terpene ozonolysis also produces highly volatile VOCs, including compounds containing at least one carbonyl functional group (Chen et al., 2021; Singer et al., 2006). For instance, D-Limonene ozonolysis has been shown to produce many carbonyl-containing VOCs products, including Levulinic acid, Maleic acid, and Limonaldehyde, all of which are shown in Figure 2 (Jaoui et al., 2006).

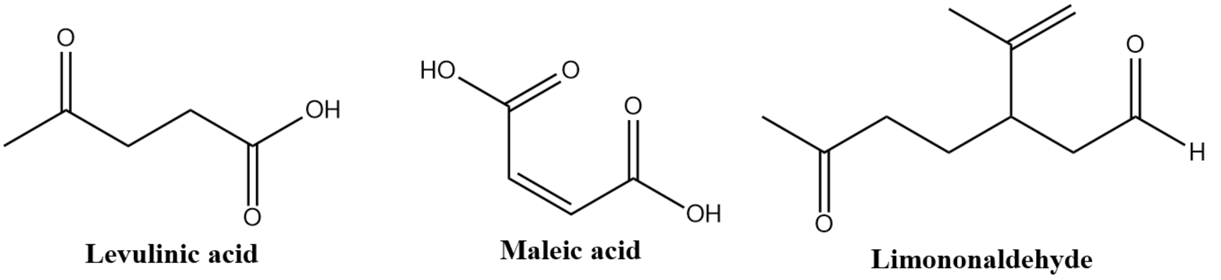

Figure 2: Several Volatile Organic Compounds (VOCs) Observed from D-Limonene Ozonolysis. (Jaoui et al., 2006)

Along with the carbonyl-containing compounds shown in Figure 2, ozonolysis products from reactions with terpene-based cleaners can produce highly volatile VOCs. Limonene is a well- known terpene present in many indoor cleaning products that reacts quickly with ozone to form highly volatile VOCs (Fiedler et al., 2005; Tamas et al., 2006). Limonene is of particular interest in indoor air quality studies because its concentrations in the typical indoor environment are quite low, but application of limonene-containing cleaners can multiply these concentrations by a factor of over one-hundred (Tamas et al., 2006). Because limonene contains two alkene groups, ozone can react with either to form VOCs. Reactions between limonene and ozone are known to occur even at high air exchange rates (Tamas et al., 2006). Limonene ozonolysis results in aldehyde formation, including formaldehyde, which is a particularly volatile organic compound (Weschler and Carslaw, 2018). Singer et al. found that the use of a terpene-containing pine-based cleaner with an ozone generator in a large chamber mimicking the size of a bedroom yielded several VOCs including acetone and formaldehyde (Singer et al., 2006). Formation of formaldehyde is consistent with proposed paths of limonene ozonolysis, suggesting that the presence of limonene in cleaning products can increase formaldehyde formation (Chen et al., 2021). Formaldehyde is of particular interest in indoor air quality studies because it is a known carcinogen and can have many other negative health effects (Huang et al., 2012). The maximum recommended exposure to formaldehyde concentration is about 2.4 ppb (Wisthaler et al., 2005). However, much higher concentrations of formaldehyde have been observed in studies conducting reactions between terpene-containing cleaners and ozone.

Chiu et al found that lemon oil, which contains high amounts of limonene, reacts with ozone in the indoor environment to generate formaldehyde with a concentration of 69 ppb, over

25x the average concentration (Chiu et al., 2009; Wisthaler et al., 2005). Since carbonyl-containing compounds like aldehydes are known to be especially volatile, these results suggest reactions of indoor cleaning products with ozone can significantly alter the quality of indoor air (Singer et al., 2006). Production of these VOCs upon reaction of commonly used indoor cleaners and ozone is of particular concern for human health.

1.4: Heterogeneous Chemistry

This study primarily sought to identify gaseous VOCs released from reactions at the air-liquid thin film interface using two methods of analysis. Figure 3 shows a scheme that demonstrates how VOCs diffuse through and react in different phases. This scheme is based on the indoor environment mimicked in this study. Limonene, the terpene present in both cleaners examined in this study, is depicted in this scheme, but most terpene products in the cleaner are expected to react similarly. When the cleaner is initially applied to a surface, the cleaner is in the liquid phase. As the cleaner dries, it undergoes diffusion and can exist in both the bulk liquid and at the liquid-gas interface, which can also be referred to as the thin film phase. As the cleaner dries, it is expected that diffusion with the quasi-liquid slows. Ozone (in the gas phase) is expected to react with the cleaner in each phase.

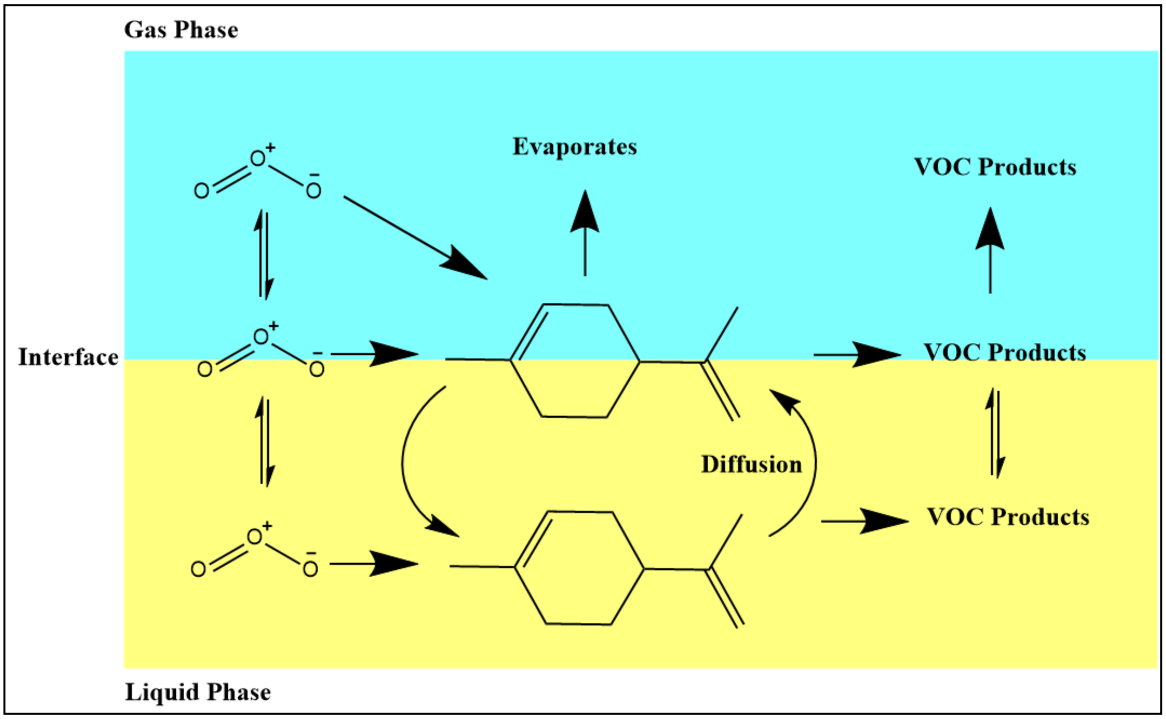

Figure 3: Surface chemistry of terpenes in cleaner in liquid, gas, and the interface between the two. This scheme is meant to mimic how the chemistry of a cleaner changes in the indoor environment.

Reactions between ozone and thin-film phase cleaners are believed to be impacted by the relative humidity of the indoor environment. When the relative humidity is high, the concentration of organic compounds persisting on surfaces has been observed to increase compared to low relative humidity environments (Markowicz and Larsson, 2015). Additionally, a thin film in a high relative humidity environment will have more water, which will cause organic compounds present within the cleaner to diffuse more quickly. Whether or not the relative humidity has an impact on VOCs present is dependent on several factors. For instance, Markowicz and Larsson observed a higher concentration of VOCs released from a wooden surface at higher humidity levels (Markowicz and Larsson, 2015). However, when gas-phase VOCs were quantified in a similar reaction, there was no change in the amount of VOCs formed at different relative humidities (Markowicz and Larsson, 2015).

Chemistry in the thin film phase frequently occurs on surfaces in the indoor environment. In contrast to gas-phase chemistry, surface chemistry is less dependent on the air exchange rate (Weschler and Carslaw, 2018). However, human exposure to VOCs in the indoor environment is believed to come mostly from products of surface reactions (Weschler, 2011). Such reactions are impacted by the amount of sorbed water present on the surface (Weschler, 2011). The relative humidity of the indoor environment has also been shown to affect the extent to which these reactions occur; environments with high relative humidity levels are believed to increase the probability of surface reactions (Weschler, 2011).

1.5: This Research

One goal of this study was to identify VOCs formed upon reaction of two common indoor cleaners (one lemon-based and one pine-based) with ozone. Both cleaners contained several terpenes of interest expected to undergo ozonolysis, which are shown in Figure 4. The lemon and the pine-based cleaner contain D-Limonene. The pine-based cleaner also contains Hexyl cinnamaldehyde. The lemon-based cleaner also contains α-Pinene. Since previous studies have observed the formation of VOCs upon ozonolysis of these terpenes (or similar terpenes), it was expected that cleaning products containing these components would yield similar VOCs.

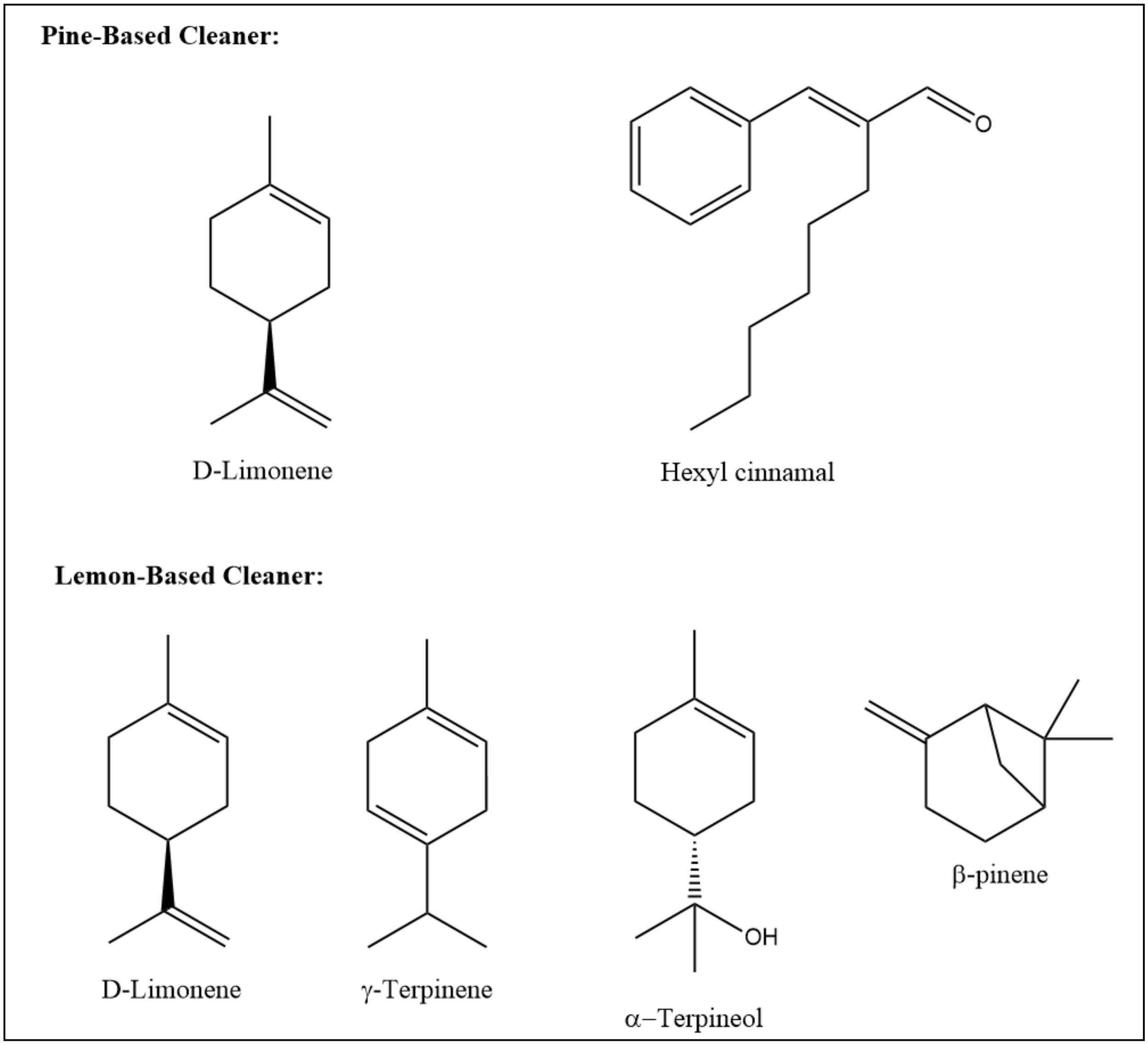

Figure 3: Terpenes Present in Pine and Lemon-Based Cleaners. The terpenes present in the pine-based cleaner were reported by the manufacturer. The terpenes expected to be present in the lemon-based cleaner are based on terpenes present in lemon oil, which is the only ingredient in the cleaner reported by the manufacturer.

Several methods can be used to conduct reactions between cleaning products and ozone. Chamber studies, such as those using bedroom or office size environments, provide a useful setup to more fully understand how these reactions actually occur in indoor environments (Singer et al., 2006; Su et al., 2007). Laminar flow reactors, although much smaller, also provide a useful way of determining compounds formed from reactions of cleaning products and ozone.

Laminar flow reactors allow for accurate calculations of ozone concentration throughout the reactions, which are used in measuring reaction kinetics. Additionally, organic compounds formed can be trapped more easily and efficiently than in a large-scale chamber. Thus, although smaller laminar flow reactors may not perfectly mimic indoor environments like larger chambers, the use of a laminar flow reactor allows for accurate determination of ozone concentrations and identification of VOCs formed, which can provide useful information about the effects of such reactions on indoor air quality.

Two methods were used in this study to identify VOCs formed from reactions of the pine- and lemon-based cleaners with ozone. The first method was used to identify VOCs in the gas phase formed from reactions of pine and lemon-based cleaners with ozone. Although VOCs formed in the gas phase are lesser in quantity than surface-VOCs, this chemistry still has an impact on indoor air quality. In particular, environments with low air exchange rates can have significant VOC formation in this phase. Additionally, some terpenes, such as limonene, undergo ozonolysis so quickly that the air exchange rate has little to no impact on VOC formation (Weschler, 2011; Wolkoff, 2007). These reactions were conducted with a laminar flow reactor with ozone provided from a UV lamp. Samples were continuously analyzed with FTIR to identify VOC formation. The second method in this study sought to identify compounds present in a thin film surface after reaction of each cleaner with ozone. To determine VOCs present in the thin film, each cleaner was applied to a ZnSe crystal connected to an attenuated total reflectance infrared spectrophotometer (ATR-IR). After drying of the cleaner, ozone was added to the system. These reactions were continuously analyzed with FTIR to identify VOCs formed. Both methods used allowed for comparison of VOC formation from reactions of each cleaner with ozone, as well as the overall impact of these cleaners on indoor air quality.

Chapter 2: Methods

2.1: Laminar Flow Reactor

Interfacial surface reactions between gaseous ozone and thin-films of cleaning products were conducted in in a laminar flow reactor. A Thermo Scientific Nicolet 6700 Fourier transform infrared spectrophotometer (FTIR) connected to the laminar flow reactor continuously monitored gaseous species exiting the laminar flow reactor, with a spectrum taken every 22 seconds. As shown in Figure 5, nitrogen gas flowed through the reactor at a rate of 2.6 standard liters per minute (sl/m) as set by the corresponding mass flow controller (MFC). A separate line also flowed from the Nitrogen through the water bubbler, which allowed for manipulation of relative humidity levels within the laminar flow reactor. Depending on the relative humidity desired, the flow rate of this tube varied. However, during all trials, the total flow rate through the tube was approximately 4000 standard cubic centimeters per minute (scc/m).

An air tank also flowed through an MFC at 1000 scc/m and through a Jelight Model 600 ultraviolet lamp as the ozone source. Since oxygen gas reacts with ozone to produce two oxygen radicals, which react with oxygen gas to form ozone, the ultraviolet lamp allowed for manipulation of ozone concentrations. The ozone source flowed through the reactor through an adjustable metal rod. As shown in Figure 4, the adjustable rod was pulled out to expose the cleaner to ozone and pushed in to remove ozone from the cleaner.

An air tank also flowed through an MFC at 1000 scc/m and through a Jelight Model 600 ultraviolet lamp as the ozone source. A mercury lamp photolyzed oxygen gas to produce two oxygen atoms, which react with oxygen gas to form ozone. The intensity of the UV light allowed for manipulation of ozone concentrations. The ozone source flowed through the reactor through an adjustable metal rod. As shown in Figure 4, the adjustable rod was pulled out to expose the cleaner to ozone and pushed in to remove ozone from the cleaner.

A removable cylindrical glass tube of length 60.5 cm and diameter 4.9 cm (Surface Area = 960.04 cm^2) was coated in one of the cleaners with a nylon brush before each reaction. To allow for an even coating along the entire tube and maximum water evaporation before the reaction began, the tube was allowed to drip vertically for approximately 10-20 minutes after application of cleaner.

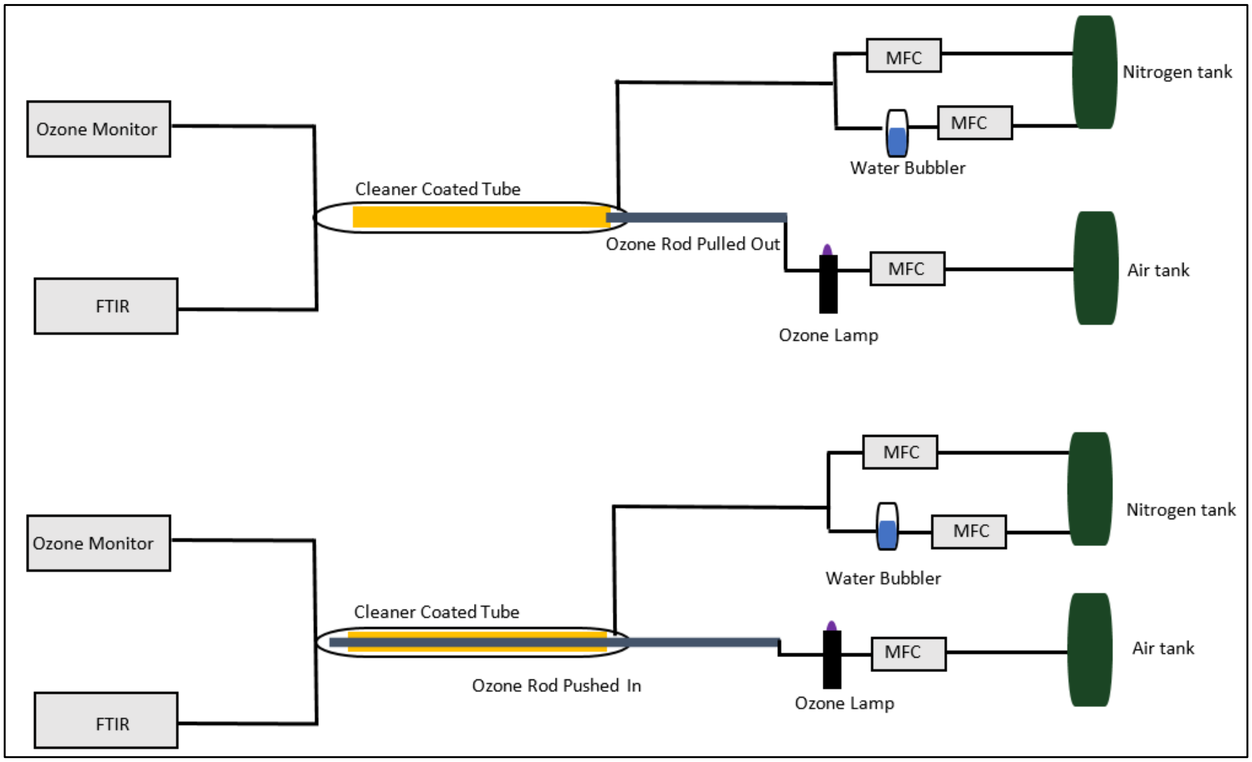

Figure 4: Laminar Flow Reactor Setup. This figure shows the flow reactor setup used for the reactions between ozone and the cleaners used.

To ensure no contaminants from previous reactions were present in the laminar flow reactor, all flows shown in Figure 4 were allowed to run for approximately twenty to thirty minutes without the cleaner coated tube and with the ultraviolet lamp providing the ozone source turned off. However, although the ultraviolet source was not turned on until later in the procedure, the air flow traveling through the ozone lamp was turned on with the other flows to mitigate changes in pressure resulting from adding an additional flow to this setup later in the reaction.

Before insertion of the cleaner coated inner tube, a background spectrum was taken with the FTIR. If contaminants were observed in the background, the flows were allowed to run for additional time. A new background spectrum was taken for each trial. A series of spectra were taken for each experiment (using OMNIC software), with a new spectrum taken approximately every 25 seconds. Upon insertion of the glass tube, spectra were taken with the ozone lamp off to allow for drying of the cleaner into a thin film state. As shown in Figure 5, while the cleaner dried, water vapor and VOCs were observed in the IR spectra collected. After most of the water vapor had evaporated as observed via IR (~20-40 minutes), the ozone lamp was turned on with the metal ozone tube pushed all the way in so that the cleaner was not exposed to ozone. This allowed for an accurate calculation of the initial ozone concentration ($[O_3]_0$).

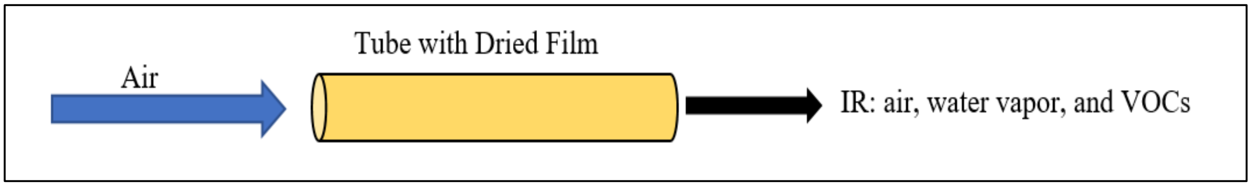

Figure 5: Cleaner Drying. While the cleaner dried to a thin film state, only air was applied.

A Model 465L UV Photometric Ozone Monitor monitored the ozone concentration every 1.00 seconds. After stability of ozone concentrations (~20-30 minutes), the metal tube was pulled out to expose the cleaner to ozone. The ozone concentrations obtained from this portion of the cycle were considered $[O_3]$. Figure 6 shows the scheme for the ozone concentrations identified as $[O_3]_t$ (where t = time in minutes) and $[O_3]_0$ (at time = 0 minutes).

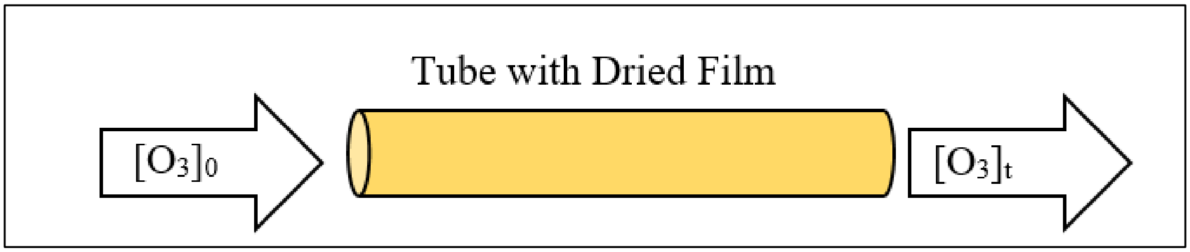

Figure 6: Ozone Concentrations Entering and Leaving Laminar Flow Reactor.

These concentrations allowed for calculation of the reactive uptake coefficient throughout the reaction, which is shown in Equation 1. This equation gives the probability that a gaseous ozone molecule colliding with a surface will lead to loss of ozone, which indicates reactivity of ozone with the compounds on the surface (Fuentes et al., 2018). In this equation, t corresponds to the time it takes a molecule of ozone to travel through the flow reactor, which is 2.628 seconds. ω_t corresponds to ozone's mean thermal velocity, and D_t corresponds to the coated tube diameter.

$$\gamma = \frac{D_t}{\omega t} ln\left(\frac{[O_3]_0}{[O_3]}\right)$$

Equation 1

2.2: Attenuated Total Reflectance Infrared Spectroscopy

Thin-film reactions between ozone and the individual cleaners were conducted with an attenuated total reflectance Thermo Scientific Nicolet 6700 Fourier transform infrared spectrophotometer (ATR-IR). With the use of OMNIC software, the IR collected a spectrum every minute. Before addition of the sample, all flows were turned on. Figure 7 shows the ATR-IR setup used in these methods. As with the laminar flow reactor setup, the flow rates for the ATR-IR setup were set by Mass Flow Controllers (MFC). Air flowed through the ozone lamp and the water bubbler (if the relative humidity was manipulated for a particular trial) to the ATR-IR chamber. Dry air also flowed through the ATR-IR chamber. The flow rates for each trial were manipulated depending on if the relative humidity was changed or not, but the total air flow throughout the chamber was 760 scc/m. This total flow rate resulted in a pressure of approximately 760 torr. Once all flows were set up and the relative humidity within the chamber stabilized, a background was taken with the ZnSe crystal. The chamber was then isolated and the crystal was removed. The ZnSe crystal was coated in the cleaner of interest and immediately added to the ATR chamber with the chamber reopened so that the flows were exposed to the ZnSe crystal. This allowed for drying of the thin film on the crystal to occur. Drying was monitored via observation of the water peak in the IR spectra.

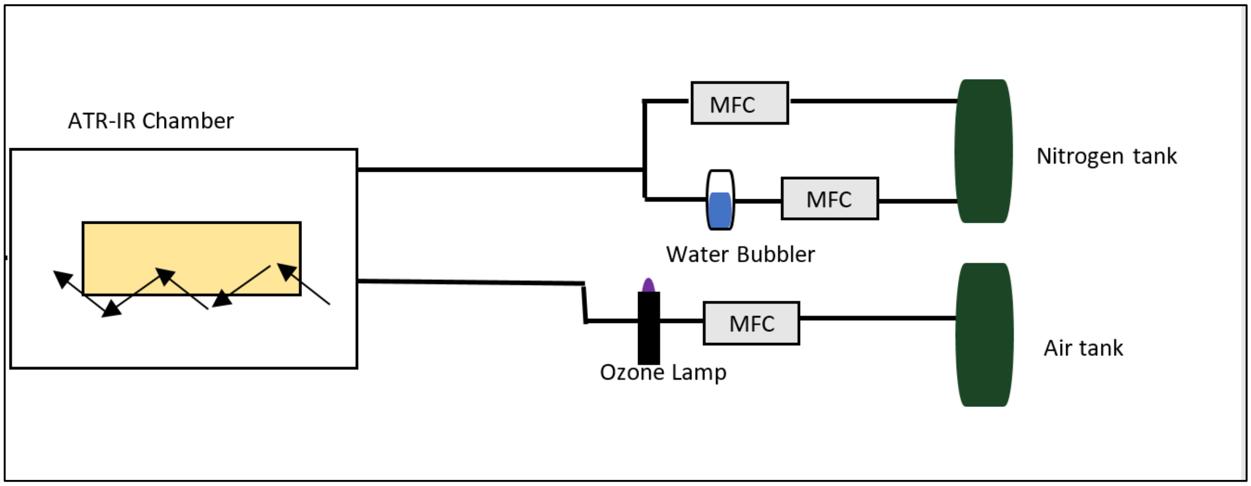

Figure 7: ATR-IR Setup Used. The ATR-IR chamber shown contains a sealed ZnSe crystal. Arrows indicate the evanescent wave traveling through the crystal resulting in the IR spectra.

Drying of the thin film on the crystal was necessary to observe components of the thin film in the IR spectra due to the ATR-IR setup. In ATR-IR, the infrared beam shines through a crystal, in this case a ZnSe crystal (Ausili et al., 2015). When the ATR-IR crystal is exposed to the infrared beam, an evanescent wave is generated. This evanescent wave (indicated in Figure 7 by the arrows) travels through the crystal and part of the sample (on the surface of the crystal) before the wave reaches the IR's detector. However, only 0.5 to 2.0 μm of the sample on the surface of the crystal can be penetrated by the evanescent wave, depending on the type of crystal used (Ausili et al., 2015). Therefore, thicker samples containing large amounts of water will not show accurate IR spectra until evaporation has occurred.

Once the water loss stopped, the chamber was isolated and the ozone lamp and monitor were turned on to allow the ozone concentration to stabilize before exposure to the cleaner. Upon stabilization of the ozone concentration, the chamber was opened to expose the cleaner to ozone. Progress of each reaction was monitored via IR using OMNIC software and analyzed with IGOR Pro software.

Chapter 3: Results and Discussion

3.1: Drying: Loss of Water Vapor and VOCs

Both the spectra obtained from gas-phase IR in the laminar flow reactor setup and the spectra obtained from ATR-IR showed significant drying for at least one hour. The early gas-phase spectra taken from the gas flow exiting the laminar flow reactor contained a large amount of highly structured absorptions in the region of 4000-3400 and 2100-1300 cm^{-1}. These peaks correspond to water vapor and make other peaks (ie, potential carbonyl or alcohol stretches) difficult to identify. In the region of 3000-2900 cm^{-1}, at least one hydrocarbon stretch is present, but the intensity of this peak is much lower than that of the water vapor, making its identification difficult. Figure 8 shows a waterfall plot illustrating the IR spectra observed while drying. The water vapor rapidly decreases; at about 60 minutes, most of the water vapor has evaporated. These spectra show that along with water vapor evaporation, VOCs are also evaporated from the flow reactor. Figure 9 shows the scheme of the reaction taking place in this environment. After a cleaner is applied to the surface (in this case the laminar flow reactor), evaporation of VOCs and water vapor occurs, with a thin film resulting minutes to hours after the application of the cleaner.

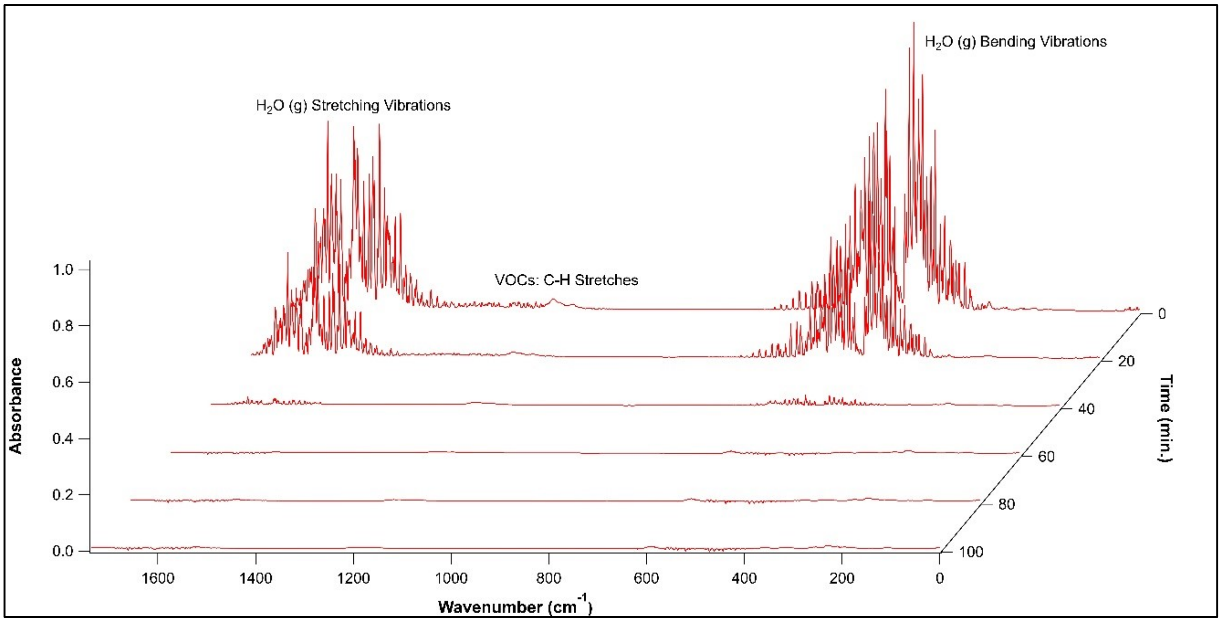

Figure 8: Waterfall Plot of IR Spectra Taken from Pine-Sol Drying in Laminar Flow Reactor. The labeled peaks show loss of water vapor and hydrocarbon VOCs.

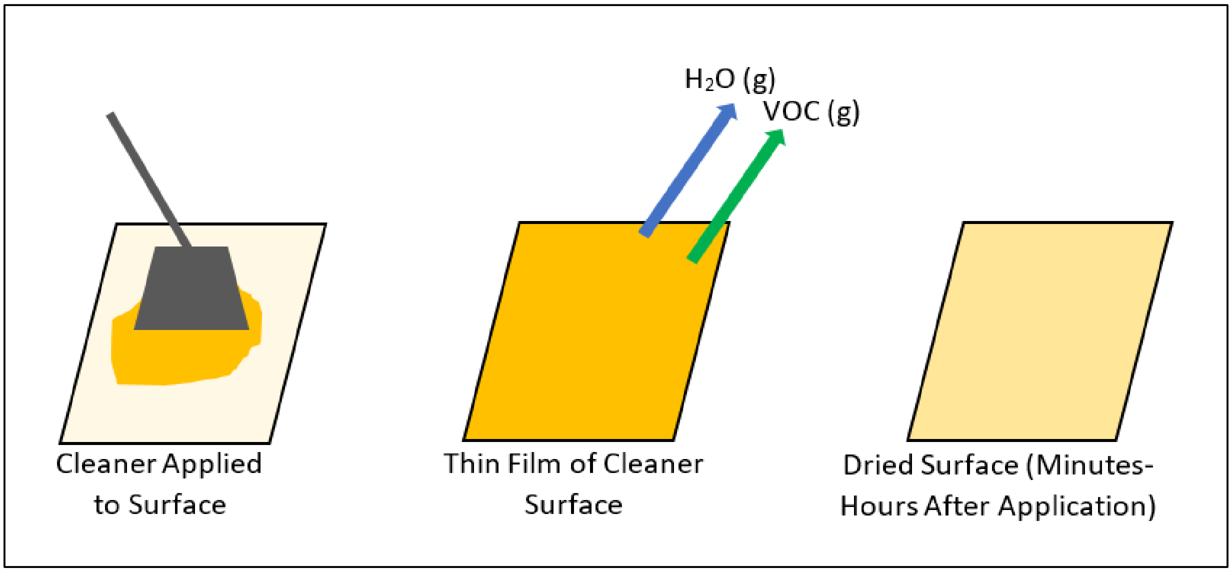

Figure 9: Environment Mimicked by Waterfall Plot (Figure 8).

To understand how this evaporation evolved over time, the water vapor IR absorption was integrated for each spectrum. The integrated absorbance values are plotted versus time in Figure 10. The integrated absorbance of the water peak for the pine-based cleaner starts at approximately 1.2 and decays to 0. However, the presence of water still prevents identification of most organic peaks until about 100 minutes. In comparison, the lemon-based cleaner contains much less water, as the initial integrated absorbance is about 0.0012. Therefore, due to the large difference in the amount of water in each cleaner, the comparative drying rates do not provide a useful comparison.

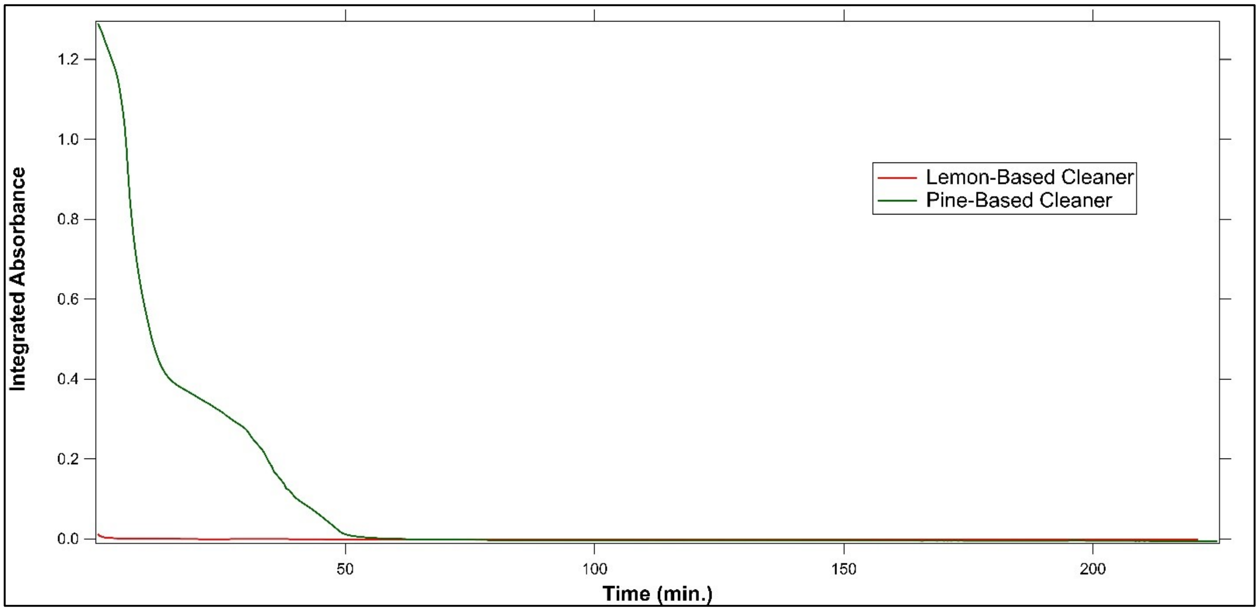

Figure 10: Integrated Absorbance of Water Peaks from Lemon and Pine-Based Cleaners in Laminar Flow Reactor. This figure shows the integrated absorbance for the lemon-based cleaner in red and the integrated absorbance for the pine-based cleaner in green.

Integration of water peaks from spectra of the thin film obtained from the ATR-IR setup are consistent with the results obtained from the gas exiting the laminar flow reactor. In the ATR-IR setup, most water loss occurred within twenty minutes of coating the cell, but drying was allowed to proceed for one hour due to continued observation of water loss, although the amount of water loss significantly decreased after the first twenty minutes. Drying samples before addition of ozone was necessary to allow the observation of organic films via IR. Upon initial coating of the cell, the film was too thick to allow the compounds present in the sample to be observed in IR. However, drying of water allowed for a more concentrated thin film. Figure 11 shows two IR spectra obtained from drying of the pine-based cleaner with the ATR-IR setup, with the corresponding vibrational modes shown in Table 1. At 1.05 minutes, the intensity of the OH stretching region is so high that the hydrocarbon peaks cannot be distinguished. There is also a water bending vibration at 1639 cm^{-1}. However, after the thin film has dried, the hydrocarbons and carbonyls are distinguishable in the IR spectrum, as the more concentrated thin film allows for penetration of the evanescent wave. Hydrocarbon stretches (wavenumbers = 2955, 2922, and 2871 cm^{-1}) and carbonyl stretches (wavenumber = 1733 cm^{-1}) indicate the presence of organic compounds from the pine-based cleaner.

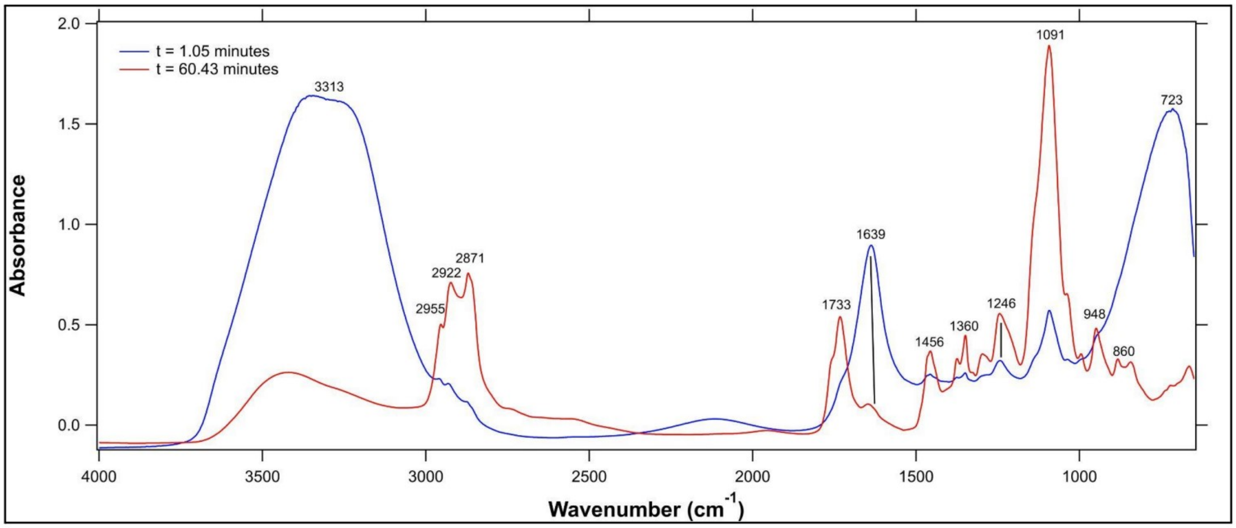

Figure 11: IR Spectra Obtained During Drying of Pine-Based Cleaner. This figure illustrates the impact of drying on IR spectra from ATR-IR by showing spectra at t = 1.05 minutes and t = 60.43 minutes.

Table 1: Vibrational Modes of Motion For IR Spectra in Figure 11.

t= 1.05 minutes		t = 60.43 minutes	
Wavenumber (cm^{-1})	Vibrational Motion	Wavenumber (cm^{-1})	Vibrational Motion
3313	OH Stretch	2955	CH Stretch
1639	OH Bend	2922	CH Stretch
		2871	CH Stretch
		1733	CO Stretch

Integration of the water and hydrocarbon peaks in the ATR-IR setup allows for comparison of loss of VOCs and water, as in the laminar flow reactor setup. Figure 12 shows the integrated absorbance of the water bending absorption the hydrocarbon stretches in Figure 11. Compared to the flow tube setup, the ATR-IR shows faster water loss. This can be seen in the marked difference in integrated absorbance. The difference can likely be attributed to the smaller amount of cleaner in the ATR-IR setup; while a flow tube reactor is large and allows for sufficient coating of a long tube, the thin film sample on a ZnSe crystal is much smaller. Figure 12 (which was obtained using ATR-IR) shows an initial integrated absorbance of 12, followed by a sharp decline with most of the water lost by 10 minutes. However, Figure 10 shows the integrated absorbance of the water peak from the pine-based cleaner at about 1.25 initially, with the value declining but not reaching zero until 50 minutes.

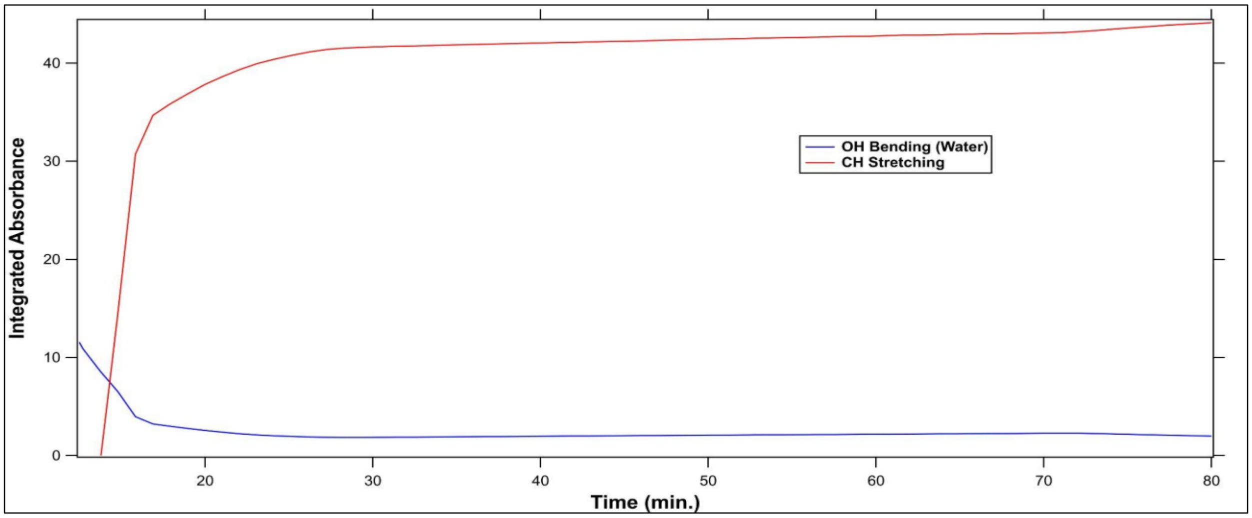

Figure 12: Integrated Absorbance of Water in Pine-Based Cleaner. This figure was obtained by integrating the alcohol stretching absorption (corresponding to water) and the hydrocarbon absorption shown in Figure 11 as obtained from the ATR-IR setup.

As in the laminar flow reactor setup, the water vapor released from the lemon-based cleaner was markedly less than in the pine-based cleaner. Figure 13 shows IR spectra from the drying period of the lemon-based cleaner. As shown in this figure, there is little to no water peak present. Additionally, there is neither a change in peak position nor intensity during the drying period. Thus, although the water loss cannot be quantified via calculating the integrated absorbance, this figure confirms that the amount of water vapor in the lemon-based cleaner is much less than the amount of water vapor in the pine-based cleaner.

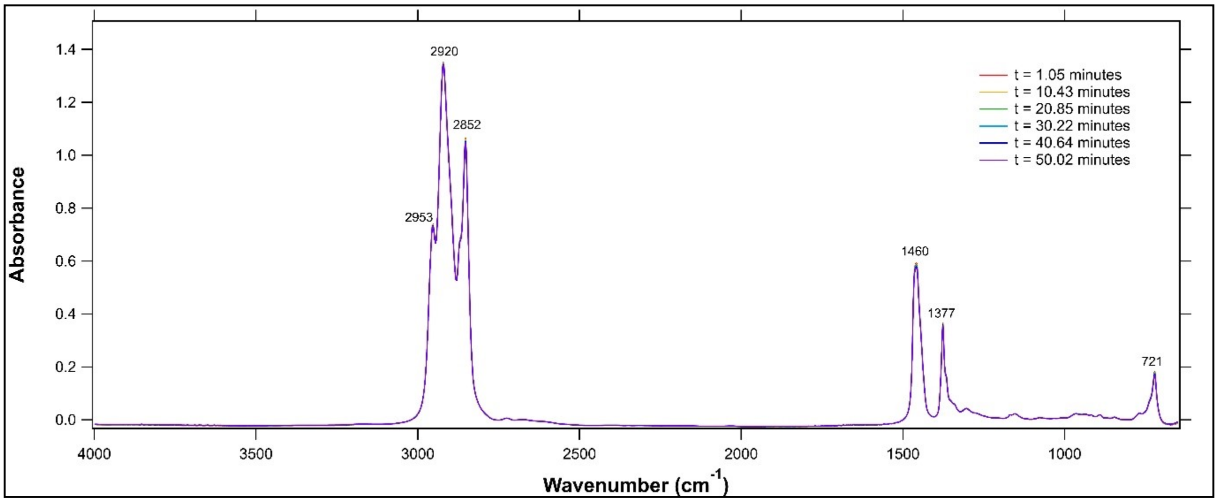

Figure 13: IR Spectra Obtained from Drying of Lemon-Based Cleaner. These spectra were obtained using the ATR-IR setup.

Along with water vapor evaporation, VOC products also evaporated from the cleaners in each trial. Figure 14 shows the integrated absorbance of a hydrocarbon stretching absorption from both the lemon and pine-based cleaner spectra obtained from flow tube reaction. As shown in this figure, the concentrations of the hydrocarbon peaks not exposed to ozone follow exponential decays. Upon exposure of each cleaner to ozone, the concentration of the hydrocarbon peaks increase, and then decrease when the ozone source is removed, which is discussed in more detail below. As shown in Figure 14, the concentration of the hydrocarbon peak from the pine-based cleaner is larger than that of the lemon-based cleaner. The integrated absorption of the hydrocarbon stretch for the pine-based cleaner is 124.14, while the integrated absorption of the hydrocarbon stretch for the lemon-based cleaner is 54.04. This suggests that the pine-based cleaner contains about double the amount of VOCs (at least in the hydrocarbon region) as compared to the lemon-based cleaner.

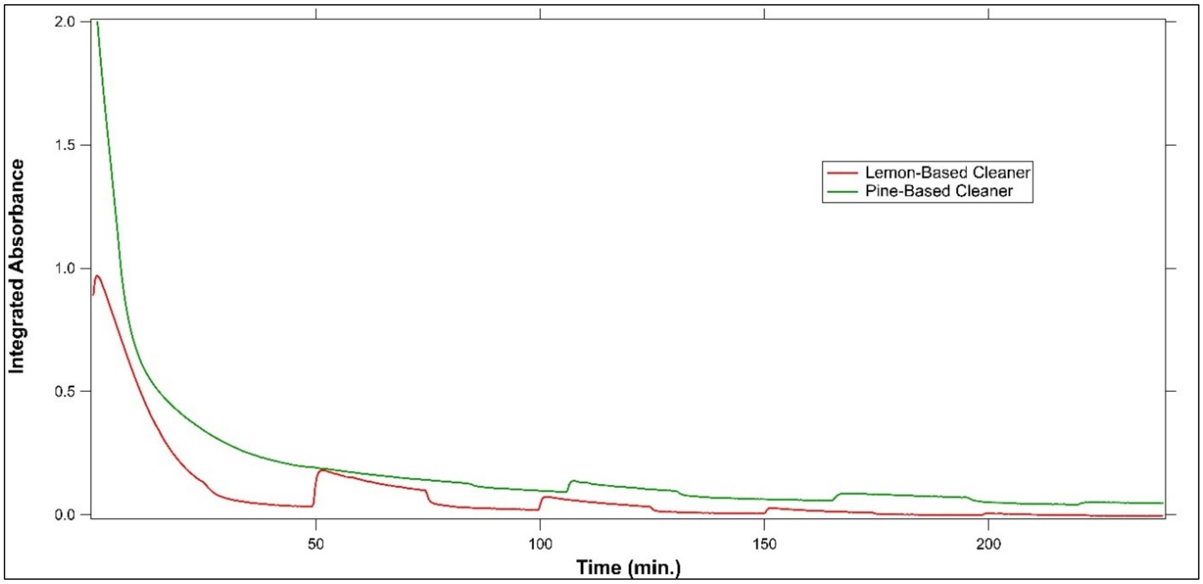

Figure 14: Integrated Absorbance of Hydrocarbon Peaks from Lemon and Pine-Based Cleaners. This figure shows the integrated absorbance of a hydrocarbon peak from both sets of spectra over the course of each reaction in the laminar flow reactor, with the lemon-based cleaner shown in red and the pine-based cleaner shown in green.

Comparatively, the loss of VOCs is less in the ATR-IR setup and occurs more quickly. Figure 12 shows that while drying in the ATR-IR setup, the pine-based cleaner loses most of its water after twenty minutes, versus one hundred minutes in the laminar flow reactor setup for the same process. However, as with water vapor loss, this smaller loss in the ATR-IR setup is likely the result of a smaller sample size. Additionally, based on Figure 13, the loss of VOCs in the lemon-based cleaner appears to be negligible. Since the laminar flow reactor setup showed faster loss of VOCs in the lemon-based cleaner than in the pine-based cleaner, this could simply be a result of less VOCs present or occurring so quickly the drying cannot be observed in the spectra.

3.2: Gaseous Ozone Concentrations and Reactivity

The ozone concentrations obtained allow for quantification of ozone reactivity with each cleaner and show how the reactivity changes while each cleaner undergoes ozonolysis. Gas-phase ozone concentrations for the laminar flow reactor experiment of a thin film of pine-based cleaner with ozone are shown in Figure 15. Time periods before 34 minutes show the ozone concentration without contact with the cleaner ($[O_3]_0$) and are approximately 200 ppb. At 34 minutes, the ozone injector rod was retracted to initiate reactions with the thin film, resulting in a drop in ozone concentration. At 54 minutes, the ozone injector rod was pushed in to cease reactions between the ozone and thin film cleaner. This resulted in an increase in ozone concentration to approximately 180 ppb. This process was repeated, resulting in a decrease in ozone concentration at 63 minutes and an increased ozone concentration at 85 minutes.

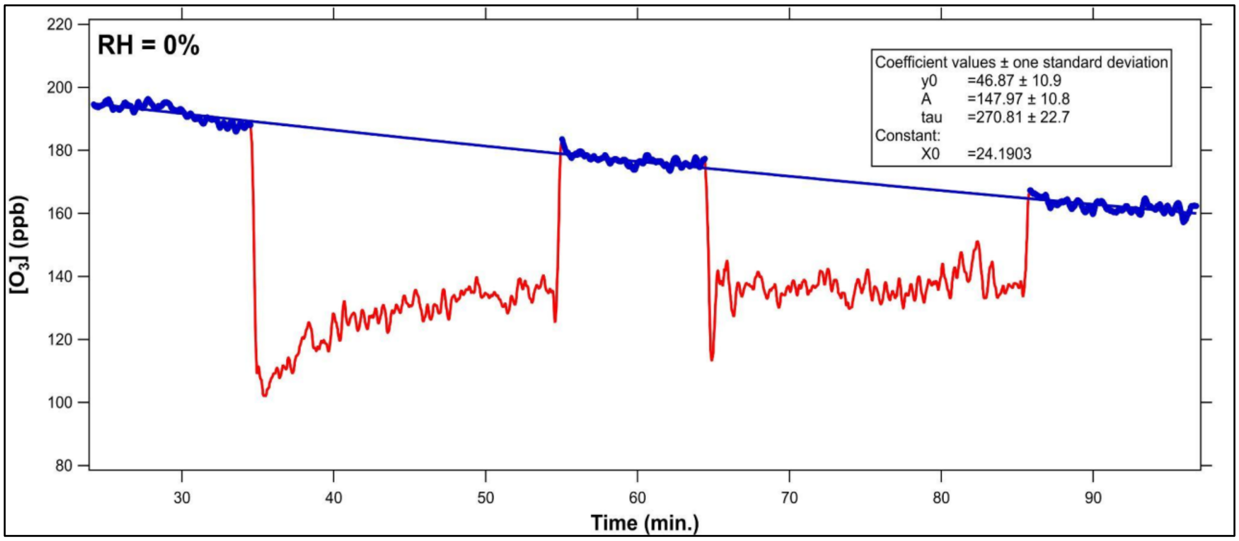

Figure 15: Ozone Concentrations During Reactions of Pine-Based Cleaner and Ozone at 0% Relative Humidity. This figure shows the concentrations of ozone over the course of the reaction upon stabilization of the initial ozone concentration ($[O_3]_0$). Periods in which the ozone was not exposed to the pine-based cleaner are shown in blue, while periods in which the ozone was exposed to the pine-based cleaner are shown in red.

As shown in Figure 15, the concentration of ozone when not exposed to the thin film cleaner decreased exponentially. Equation 2 gives the corresponding fit for this exponentially decay. This equation allows for extrapolation of the concentration of ozone when not exposed to the thin film cleaner ($[O_3]_0$) for use in Equation 1, which gives the probability that an ozone collision with the surface will result in loss of ozone.

$$[O_3]_0 = 175.32 + 32.236\left\{\frac{-(t-14.4667}{40.861}\right\} \qquad \textbf{Equation 2}$$

Figure 16 shows the concentration of ozone during the reaction of the lemon-based cleaner with ozone. The initial ozone concentration in the absence of the lemon-based cleaner was approximately 230 ppb. At 22 minutes, the adjustable rod containing the ozone source was retracted to expose of the lemon-based cleaner to ozone, this concentration dropped to approximately 150 ppb. At 42 minutes, the retractable rod was pushed in to cease this reaction, and the ozone concentration increased to approximately 210 ppb. This cycle was repeated; at 52 minutes, the ozone rod was retracted and at 72 minutes, the rod was pushed in to end the reaction between the cleaner and ozone. As with the pine-based cleaner, the concentration of ozone not exposed to the lemon-based cleaner followed a path of exponential decay, which is shown in the blue line of fit in Figure 16. The resulting equation allows for calculation of $[O_3]_0$ over the course of the reaction, which can be used in Equation 1 to calculate the effective uptake coefficient.

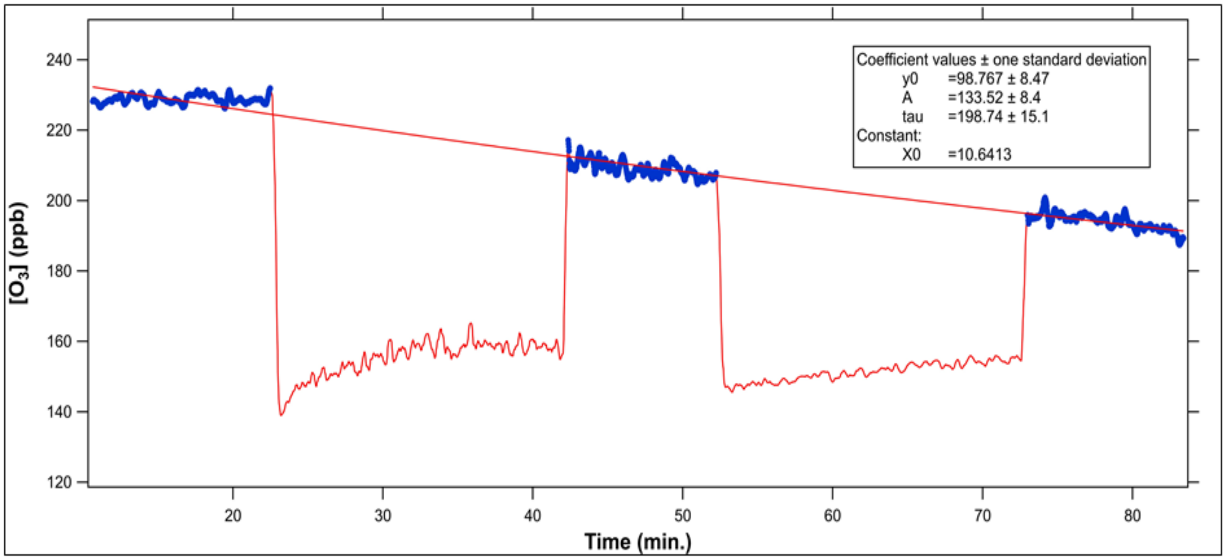

Figure 16: Ozone Concentrations During Reaction of Lemon-Based Cleaner and Ozone. This figure shows the concentration of ozone over the course of the reaction upon stabilization of the initial ozone concentration ($[O_3]_0$). Periods in which the ozone was not exposed to the lemon-based cleaner are shown in blue, while periods in which the ozone was exposed to the lemon-based cleaner are shown in red.

In order to compare the reactivity with ozone of the lemon and pine-based cleaners, the effective uptake coefficients were calculated for the data from Figures 15 and 16 using Equation 1. Figure 16 shows the effective uptake coefficients for the lemon and pine-based cleaners at 0% RH. As shown in this figure, the reactivities of both cleaners with ozone are relatively equal. This is likely due to their similar chemical compositions; both cleaners contain limonene and other terpenes known to undergo ozonolysis. Additionally, the similar reactivities with ozone suggest similar concentrations of reactive components.

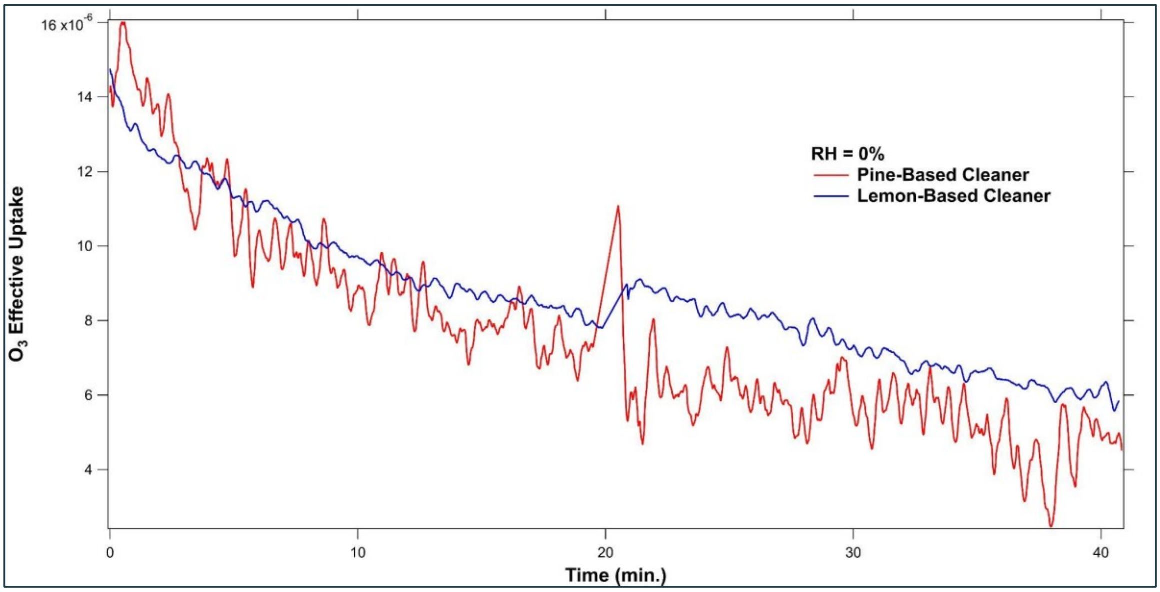

Figure 16: Effective Uptake Coefficients at 0% RH for Lemon and Pine-Based Cleaners. These values were calculated using the data from Figures 15 and 16 and Equation 1. This figure shows the effective uptakes from the first and second exposure of the cleaners to ozone spliced together, which accounts for the slight uptick at approximately twenty minutes.

Figures 17 and 18 show the effective uptake coefficients for the lemon and pine-based cleaners (respectively) at 0% and 62% relative humidities over two exposure cycles to ozone. For the first exposure cycle (0 to 20 minutes), the effective uptake of ozone in the lemon-based cleaner (Figure 18) is slightly higher at 0% RH than 62% RH. This difference is likely negligible. For the second exposure, the relative humidities show no significant difference in effective uptake. The pine-based cleaner (Figure 17) shows no difference in effective uptake of ozone at different relative humidities. Most literature suggests that under higher relative humidity conditions, the probability of terpene ozonolysis on surfaces increases due to the presence of sorbed water (Weschler, 2011; Markowicz, 2015). However, as shown in Figures 17 and 18, this is not necessarily the case for gaseous products. Fu et al. reported no difference in reactivity of squalene (a terpene) with ozone on surfaces at different relative humidity levels (Fu et al., 2013). However, this is likely due to the decreased reactivity of squalene with ozone as compared to limonene (Fu et al., 2013). In contrast, Markowicz et al. found that as relative humidity increased in the indoor environment, the amount of VOCs on both surfaces and in the gas phase increased as well (Markowicz et al., 2015). However, Markowicz et al. did not focus on the reactivity of specific compounds, but rather the amount and identification of VOCs present. The results of this study suggest that ozone loss does not change at higher relative humidity levels. One limitation of the experimental setup was the lack of continuous ozone monitoring for the ATR-IR setup, but future studies should examine effective uptake coefficients for surface reactions of cleaners to determine if these values are significantly different than the gas phase effective uptake coefficients.

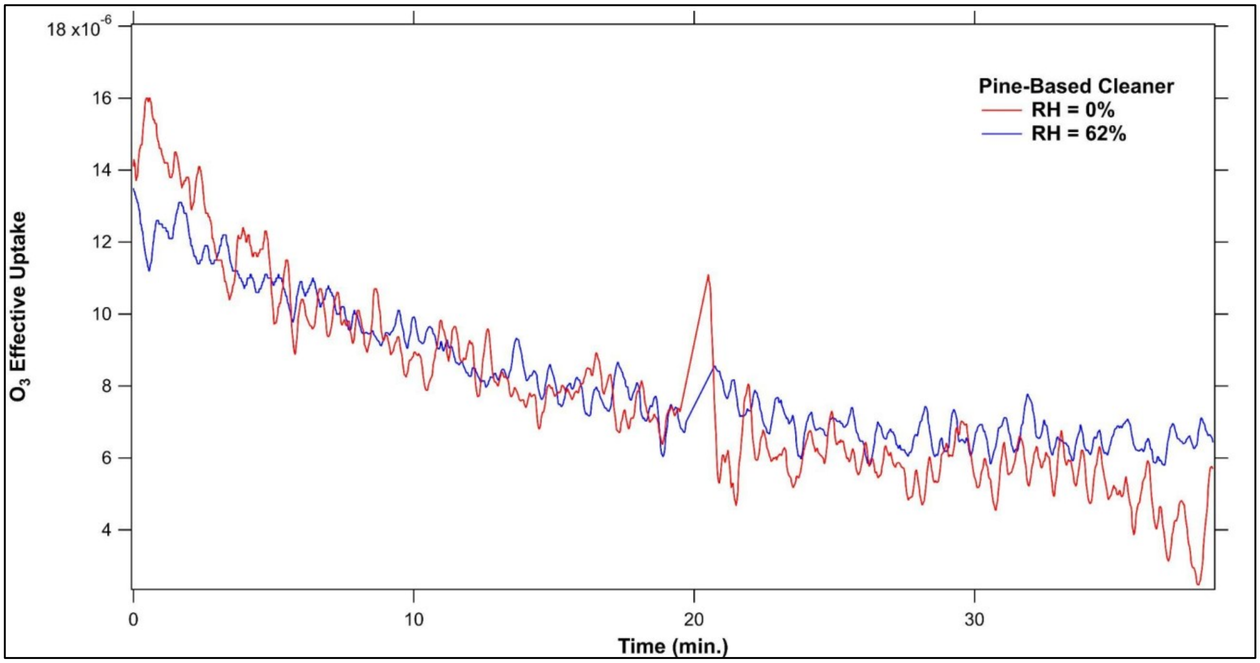

Figure 17: Effective Uptake Coefficient of Pine-Based Cleaner at 0% and 62% RH. This figure shows the effective uptake coefficient of ozone for the pine-based cleaner at 2 relative humidities. The effective uptakes from the two exposures are spliced together, which accounts for the uptick at approximately twenty minutes.

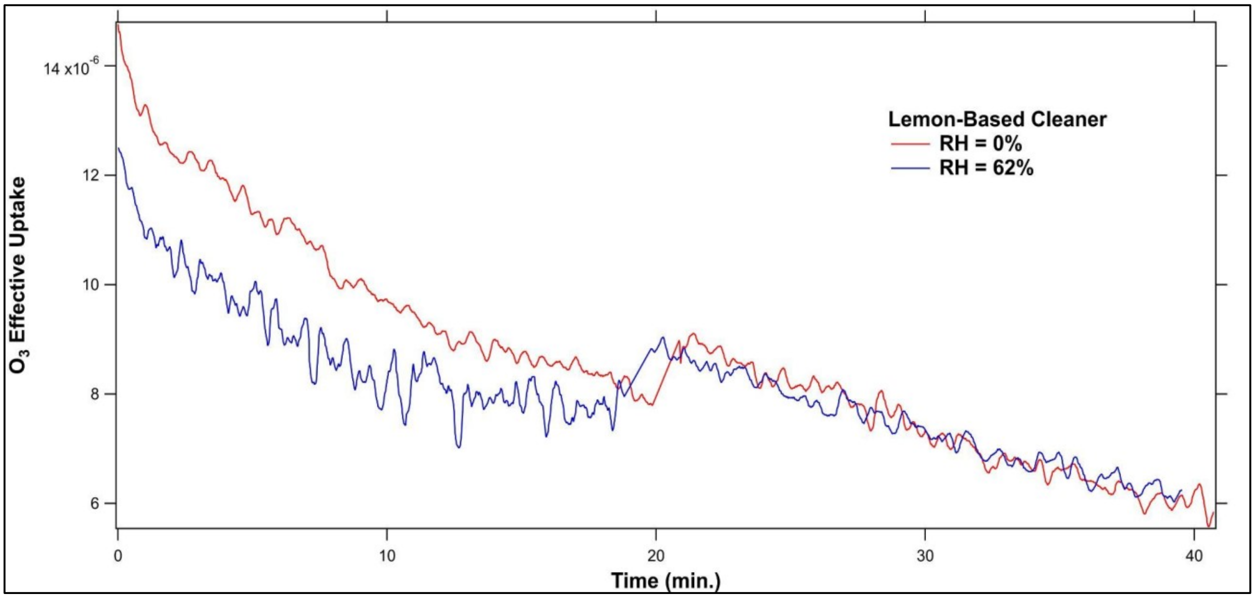

Figure 18: Effective Uptake Coefficient of Lemon-Based Cleaner at 0% and 62% RH. This figure shows the effective uptake coefficient of ozone for the lemon-based cleaner at 2 relative humidities. The effective uptakes from the two exposures are spliced together, which accounts for the uptick at approximately twenty minutes.

3.3: VOC Products Observed in IR Spectra

IR spectra obtained from both methods showed the presence of VOC signals corresponding to products upon exposure of the cleaners to ozone. The VOCs released different signals in the IR spectra than in the initial spectra showing just the cleaner. Integrated IR spectra allowed for the calculation of concentrations of new products over the course of the reaction. As shown in Figure 19, the intensity of the hydrocarbon peak increases upon exposure of the pine-based cleaner to ozone. The concentration of the hydrocarbon peak corresponding to no ozone exposure follows a line of exponential decay. The resulting equation is Equation 2.

$$[VOC]_t = 0.023465 + 0.074952\left\{\frac{-(t-98.6)}{82.456}\right\}$$ **Equation 2**

As shown in Figure 19, upon addition of ozone, the concentration of the hydrocarbon peak increases, while the concentration of the hydrocarbon peak decreases upon removal of ozone. The same method of analysis on two other peaks of interest, one in the alcohol region and one in the carbonyl region, showed that new products also formed in these regions upon exposure of the pine-based cleaner to ozone.

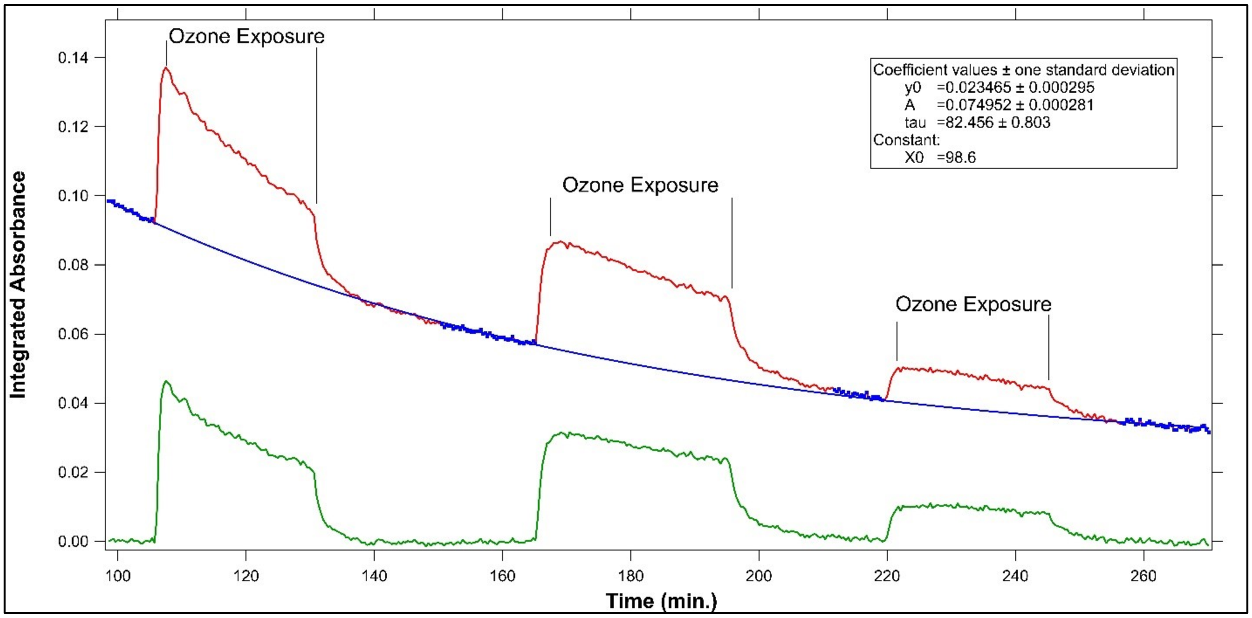

Figure 19: Integrated Absorbance of Hydrocarbon Peaks from Pine-Based Cleaner. This figure plots a line of exponential decay corresponding to the concentration of the peak not exposure to ozone. This peak is subtracted out to give the signal of the hydrocarbon product (green). The IR spectra used to calculate these values were obtained from the flow tube setup.

Figure 20 shows the hydrocarbon, alcohol, and carbonyl signals obtained from the method of analysis illustrated in Figure 19. As shown in this figure, the intensity of the hydrocarbon peak is the highest, followed by the carbonyl peak and the alcohol peak. While the hydrocarbon peak appears to decrease in intensity over time (which can be attributed to expected VOC loss/reactions of products with hydroxyl radicals and ozone), the carbonyl and alcohol peaks appear to be highest in the second cycle of cleaner exposure to ozone. This difference is likely due to the intermolecular forces present in the different VOC products. Hydrocarbon products are likely the smallest and have the highest volatility. Their intermolecular forces are also markedly weak, as London dispersion are the main force in these compounds. In contrast, carbonyl compounds have dipole-dipole interactions (along with London dispersion forces), suggesting that these compounds are not observed as quickly. As shown in Figure 20, the highest concentration of carbonyl products appears in the second exposure cycle. OH-containing compounds are expected to have the stronger intermolecular forces due to Hydrogen bonding (along with dipole-dipole and London dispersion forces). Thus, it is unsurprising that the integrated absorbance of the OH-containing compounds is lowest and does not have the highest intensity until later in the reaction.

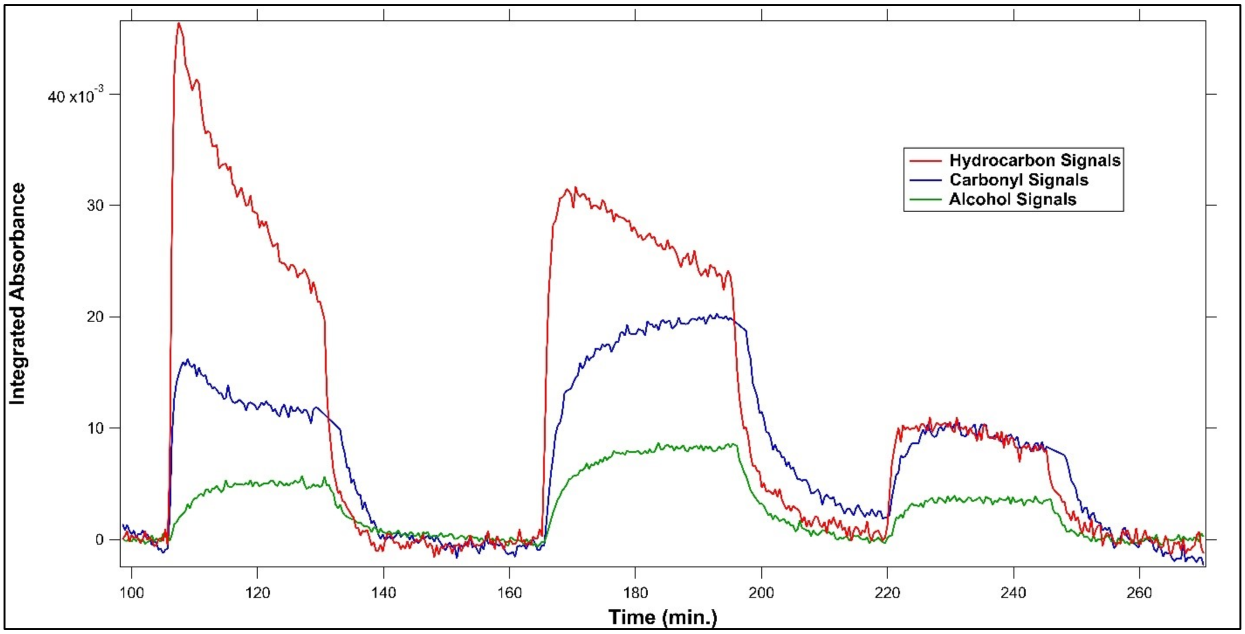

Figure 20: Signals Obtained From Reaction of Pine-Based Cleaner With Ozone in Laminar Flow Reactor. These signals were obtained from integrated absorbances of IR spectra (method of analysis shown in Figure 19).

However, while the integrated absorbances may provide some indication as to what products are formed, the intensity of absorbance is somewhat nuanced. The hydrocarbon signal is largest in integrated absorbance due to the fact that hydrocarbon functional groups are also present in OH and carbonyl-containing products. Furthermore, although integrated absorbance does provide some information about the amount of product formed, since the molar absorptivity is not known, these peaks do not directly correlate to concentration. Therefore, although these integrated signals do not directly indicate concentration of products, these results do show that upon exposure to ozone, they do provide insight as to the functional groups present in products formed throughout the reaction.

Ultimately, these functional group products result in at least two unique IR spectra for the reaction of the pine-based cleaner with ozone. Figure 21 shows two difference spectra obtained from the reaction of the pine-based cleaner with ozone. Each spectrum was taken soon after addition of ozone, with the spectrum taken just before addition of ozone subtracted out. Corresponding peaks of interest for each spectrum, as well as the spectrum obtained for the lemon-based cleaner, are identified in Table 2. As shown in this figure, the concentration of the hydrocarbon products decreases over the course of the reaction. However, the carbonyl and OH products increase at the second ozone exposure. This suggests that at the beginning of the reaction, the VOC product(s) contains hydrocarbon and carbonyl functional groups. Later in the reaction, VOCs contain hydrocarbon, carbonyl, and OH functional groups. Although the hydrocarbon and carbonyl groups are present in both products, the change in peak shape suggests that new compounds containing these functional groups, as well as OH functional groups, are present later in the reaction.

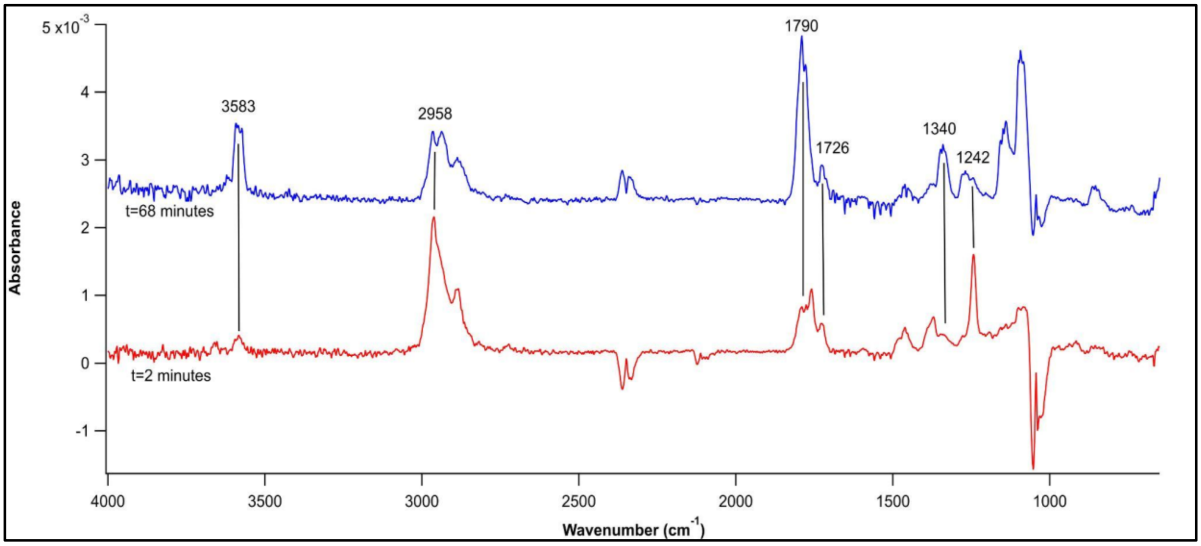

Figure 21: Difference IR Spectra of Pine-Based Cleaner and Ozone. These two spectra were obtained at two different points of the reaction. The 2 minutes (red) spectrum was taken soon after initial exposure of ozone to the pine-based cleaner, while the 68 minutes (blue) spectrum was taken after two exposures of the pine-based cleaner to ozone. The corresponding spectrum not exposed to ozone was subtracted from each to ensure the products were from reactions of VOCs and ozone and not VOCs already present in the cleaner.

Table 2: Identified Peaks and Vibrational Motion From IR Spectra From Pine and Lemon-Based Cleaners. The corresponding spectra are shown in Figures 21 and 22.

	Pine-Based Cleaner (t=2 minutes)	**Pine-Based Cleaner (t=68 minutes)**	**Lemon-Based Cleaner**
Vibrational Motion	**Wavenumber (cm^{-1})**	**Wavenumber (cm^{-1})**	**Wavenumber (cm^{-1})**
OH Stretch	----	3583	----
CO Stretch	1790, 1726	1790, 1726	1743, 1650
CH Stretch	2958	2958	2930

A well-defined absorbance in the spectrum taken at 2 minutes is present at approximately 2950 cm^{-1} which falls in the hydrocarbon region. This spectrum also contains an absorbance at approximately 1750 cm^{-1}, which is in the carbonyl region. Thus, a product containing hydrocarbon and carbonyl functional groups is produced soon after exposure of the pine-based cleaner to ozone. This is consistent with other studies that have observed VOC production upon exposure of VOC-containing products to ozone. Chiu et al. observed the formation of several VOCs upon reaction of essential oils containing monoterpenes and ozone, including toluene, benzene, and styrene (Chiu et al., 2009). Additionally, in a study looking at a pine-based cleaner specifically, Destaillats et al. observed the formation of aldehyde-containing compounds, including formaldehyde (Destaillats et al., 2006). Wells observed the formation of several different carbonyls and carboxylic acids from terpene ozonolysis (Wells, 2012). One such product was 2,2,4-Trimethyl-3-oxovaleraldehyde, the structure of which is shown on the right. Figure 22 shows the IR spectrum obtained at 2 minutes overlaid with a literature IR spectrum of 2,2,4-Trimethyl-3-oxovalderaldehyde (National Institute of Standards and Technology). Both spectra have peaks at similar wavenumbers in the hydrocarbon, carbonyl, and fingerprint regions of the spectra. Although the shape of some of the peaks observed in the spectrum obtained from the reaction of the pine-based cleaner with ozone slightly differ, this was not a pure sample, so the presence of other compounds in the sample affects the peak shape and intensity slightly. However, based on overall similarity of IR spectra,

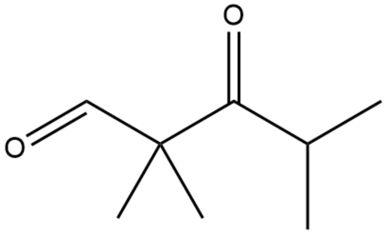

2,2,4-Trimethyl-3-oxovaleraldehyde

the IR spectrum obtained from the pine-based cleaner at 2 minutes is believed to contain this compound in a mixture consisting of several organic compounds.

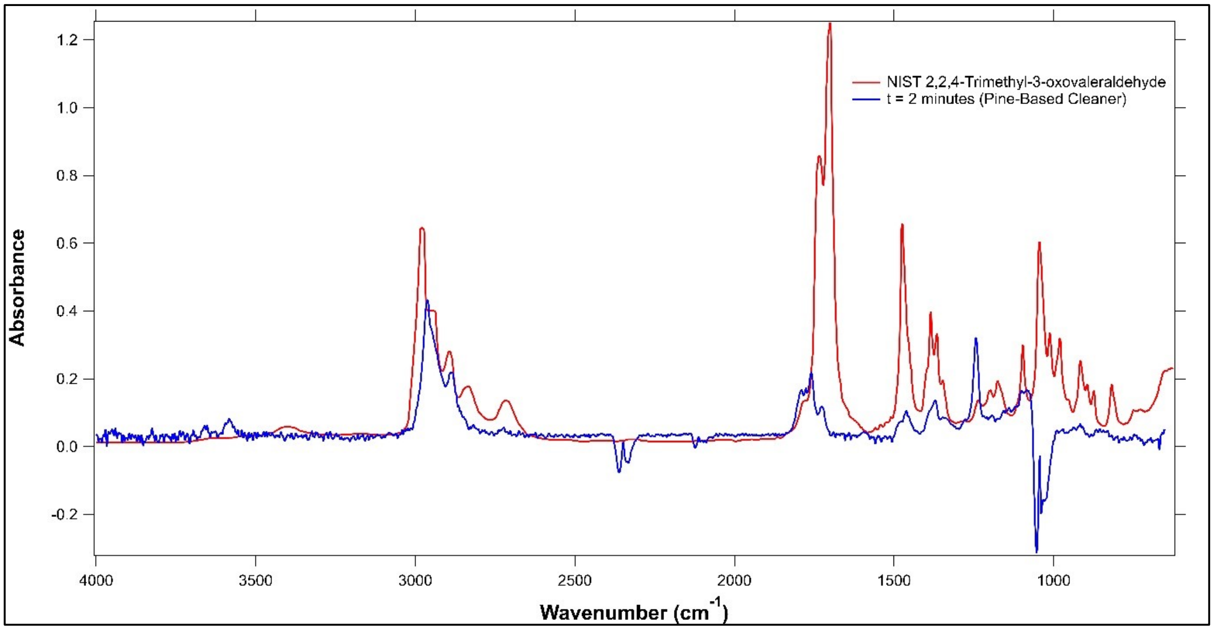

Figure 22: Difference Spectrum of Pine-Based Cleaner with Ozone Reaction Overlaid on a Spectrum of 2,2,4-Trimethyl-3-oxovaleraldehyde. The spectrum of 2,2,4-Trimethyl-3-oxovaleraldehyde was obtained from the National Institute of Standards and Technology's Chemistry Webbook.

Due to formaldehyde formation in similar reactions of terpene-containing cleaners with ozone, the IR spectrum of formaldehyde was also compared to experimental spectra. Both spectra obtained from the reaction of the pine-based cleaner with ozone, as well as a literature formaldehyde spectrum, are shown in Figure 23. Although these three spectra all show compounds with hydrocarbon and carbonyl functional groups, the precise wavenumber, intensity, and number of peaks differs among the spectra. Therefore, although aldehyde formation was observed, no significant quantity of formaldehyde was produced. This was unexpected, as formaldehyde is a known product of limonene ozonolysis (Chen et al., 2021). However, although this specific aldehyde was not formed, a different volatile aldehyde compound was formed. Therefore, the formation of this compound in the indoor environment suggests that the reaction of the pine-based cleaner with ozone will have negative effects on indoor air quality.

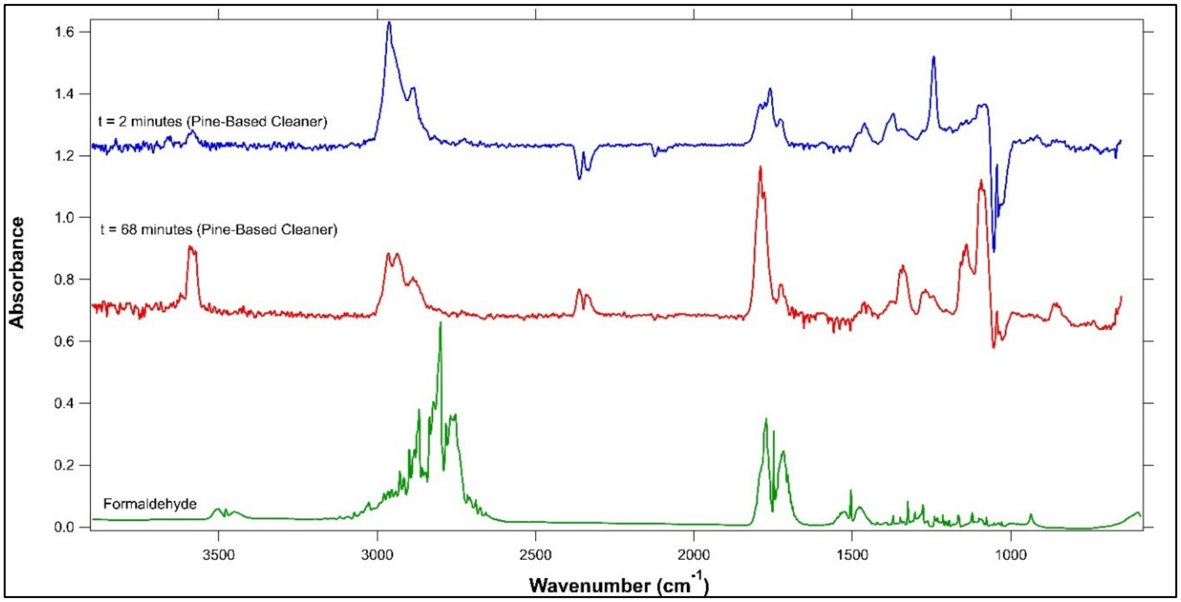

Figure 23: Difference Spectra of Pine-Based Cleaner with Ozone Reaction and Literature Spectrum of Formaldehyde. The spectrum of formaldehyde was obtained from the National Institute of Standards and Technology's Chemistry Webbook.

Limonene ozonolysis is a complex multi-step and multi-pathway that can lead to formation of many products. Limonene has two alkenes which can undergo ozonolysis. The endocyclic alkene in limonene undergoes ozonolysis at a rate approximately ten to fifty times that of ozonolysis of limonene with the exocyclic alkene (Chen et al., 2021; Ramasamy et al., 2021). Additionally, limonene ozonolysis produces hydroxyl radicals, which are known to react with organic compounds, which can produce additional VOCs (Piletic et al., 2022). As shown in Figure 24, when ozone reacts with limonene's exocyclic alkene, the reaction generates a primary ozonide intermediate. This primary ozonide then can become one of two Criegee intermediates, both of which are shown in Figure 22 (Chen et al., 2021).

Although the exocyclic pathway of limonene ozonolysis is much slower, this pathway is still significant in the indoor environment when it comes to cleaning products, which tend to persist in the indoor environment long after initial application (Chen et al., 2017). The exocyclic pathway (Figure 22) also generates a primary ozonide (Chen et al., 2021). From here, limona ketone, a minor product, is formed (Donahue et al., 2007). Although limona ketone is considered a product of limonene ozonolysis, it is reactive with other components in the indoor environment and can generate secondary organic aerosols (SOA), a subclass of fine particulate matter that is of particular concern for human health with defined levels of “safe” concentrations (Donahue et al., 2007). The exocyclic primary ozonide also forms an additional Criegee intermediate. Although this Criegee intermediate contains two radicals, the same number as the endocyclic Criegee intermediates do, the exocyclic Criegee intermediate contains one fewer oxygen (Chen et al., 2021). This is due to the formation of formaldehyde upon breakdown of the exocyclic primary ozonide (Chen et al., 2021). Formation of the Criegee intermediate and formaldehyde is more favorable than the limona ketone product (Witkowski et al., 2018). Unfortunately, 2,2,4-Trimethyl-3-oxovalderaldehyde is a relatively newly identified limonene ozonolysis product, and thus a mechanism leading to its formation has yet to be determined.

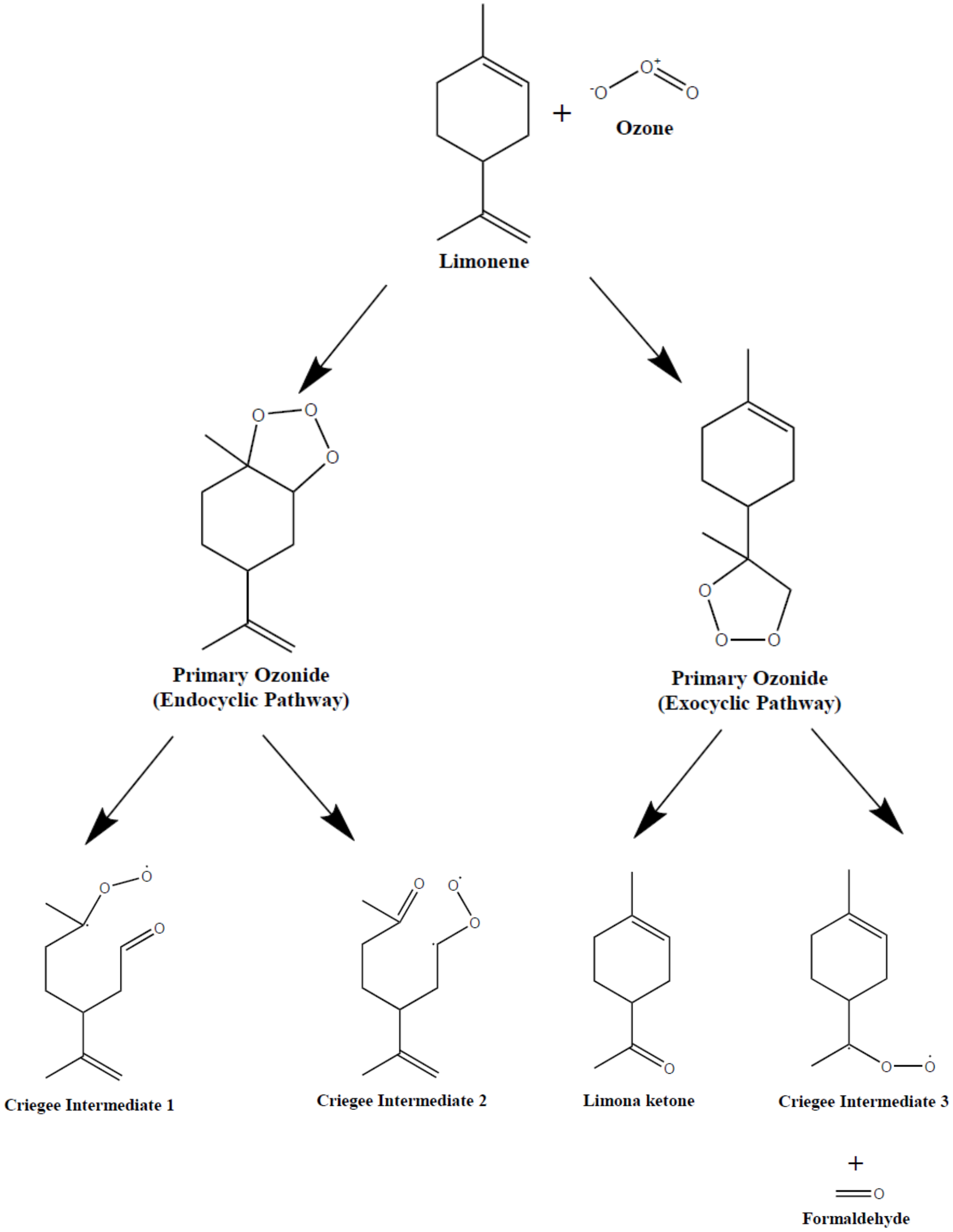

Figure 24: Endocyclic and Exocyclic Pathways of Limonene Ozonolysis. The endocyclic pathway of limonene ozonolysis results in the formation of a primary ozonide followed by two Criegee intermediates. The exocyclic pathway results in the formation of a different primary ozonide followed by formation of an additional Criegee intermediate as well as limona ketone (Chen et al., 2021).

The lemon-based cleaner also showed increased concentrations of organic compounds upon exposure to ozone. Figure 25 shows the integrated absorbance of products from several peaks of interest in the IR spectra of the lemon-based cleaner. The compounds were identified via the same method shown in Figure 19. In contrast to the pine-based cleaner, only two peaks of interest were present in the IR spectra, one in the hydrocarbon region and one in the carbonyl region. Additionally, as shown in Figure 25, both the products decayed over the course of the reaction. This differs from the results from the pine-based cleaner (Figure 20), which show an increase in carbonyl and alcohol peaks later in the reaction. Thus, it is likely that the lemon-based cleaner does not produce new products later in the reaction.

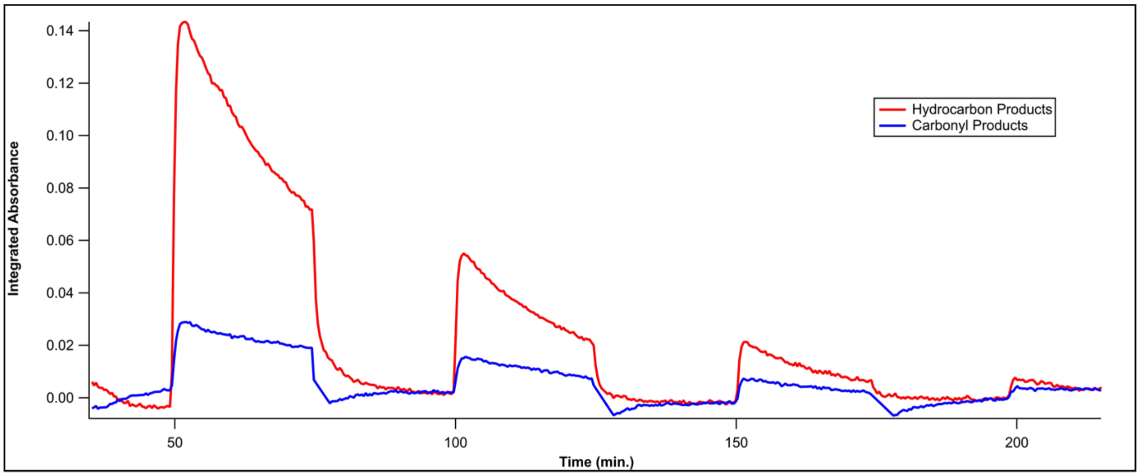

Figure 25: Integrated Absorbance of Hydrocarbon and Carbonyl Peaks from IR Spectra of Lemon-Based Cleaner. This figure shows the integrated absorbance corresponding to the products of each peak of interest using the method of analysis shown in Figure 19.

Although Figure 25 shows the growth of organic compounds in the hydrocarbon and carbonyl regions, these are not necessarily new compounds produced. Unlike the pine-based cleaner, the lemon-based cleaner does not show the growth of new organic compounds over the course of the reaction. Figure 26 shows several difference IR spectra of the lemon-based cleaner reacting with ozone throughout the exposure period obtained from subtracting out a spectrum of the lemon-based cleaner without ozone. The peaks in each spectrum change in intensity throughout the reaction. As shown in Table 2 and Figure 26, the peak at 3083 cm^{-1} likely corresponds to a hydrocarbon peak. Although this peak is clearly present in the first spectrum obtained at 51.62 minutes, the intensity of this spectrum decreases and cannot be seen in later spectra. The peak at 2930 cm^{-1} also corresponds to a hydrocarbon peak. As shown in the spectrum obtained at 51.62 minutes, the peak is initially very intense. In later spectra, this peak decreases in intensity, with only a small peak present at 199.69 minutes. However, this peak generally maintains the same shape, suggesting that only one product is present throughout the reaction. Carbonyl peaks present at 1743 cm^{-1} and 1650 cm^{-1} display the same trend, with intensity but not shape changing over the course of the reaction. The fingerprint region also follows this trend. Although there are definitely increased concentrations of organics, these compounds are unlikely to be new products. Figure 27 shows the hydrocarbon region from one of the difference spectra in Figure 26 and a spectrum of the lemon-based cleaner during drying (before ozone exposure). These spectra show such marked similarity in hydrocarbon signal that they are likely the same product. Compounds in the carbonyl and fingerprint regions are not as easily identifiable in the spectrum obtained during drying due to water vapor. However, this similarity suggests that upon reaction with ozone, the lemon-based cleaner does not form new products, unlike the pine-based cleaner, but that ozone causes an increase in concentration of compounds already present.

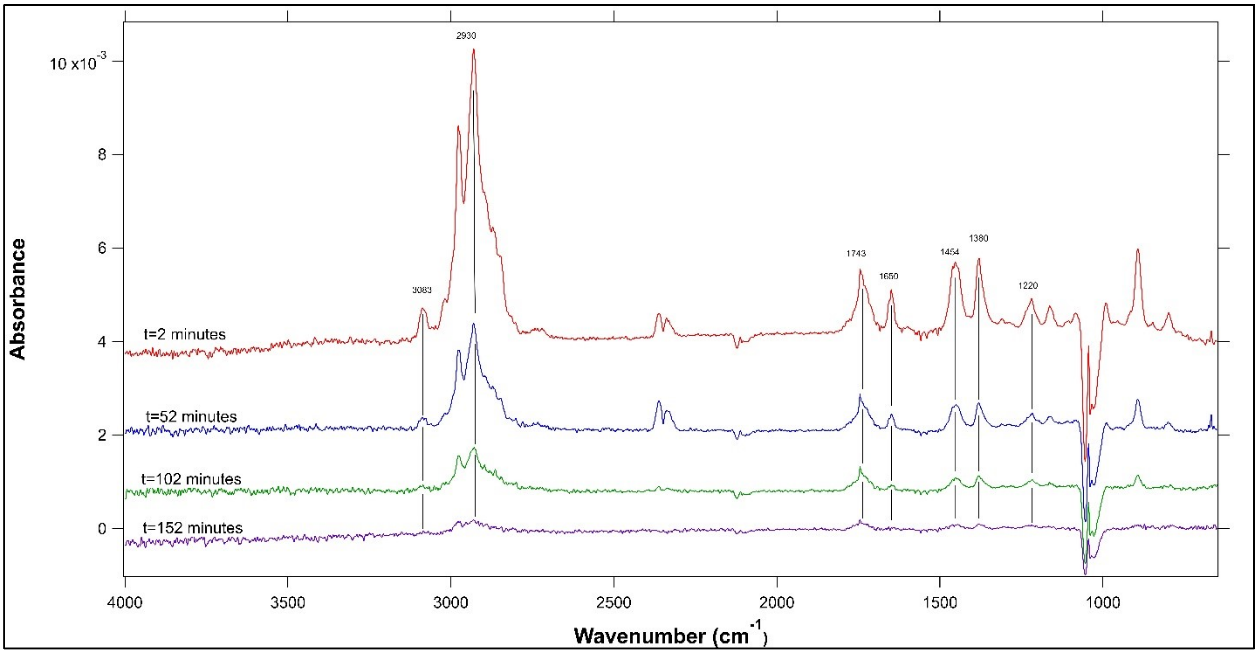

Figure 26: Difference IR Spectra of Lemon-Based Cleaner and Ozone. These four spectra were obtained at different points of the reaction. Each spectrum corresponds to a different cycle of exposure to ozone.

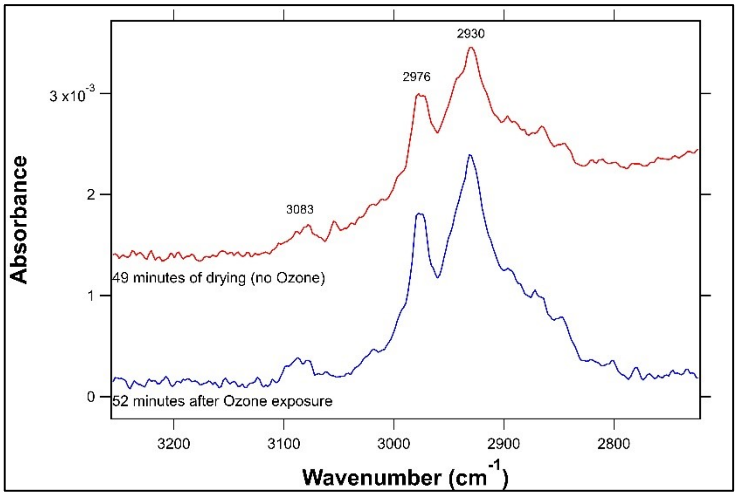

Figure 27: Hydrocarbon Signals from IR Spectra of Lemon-Based Cleaner With and Without Ozone Exposure.

The trials conducted with the ATR-IR setup also showed growth of organic peaks as in the IR spectra. Figure 28 shows spectra over 240 minutes obtained from the reaction of the pine-based cleaner with ozone in the thin film phase. However, compared to the laminar flow reactor setup, the ATR-IR setup showed more consistency in peak intensity and position. The difference spectra corresponding to these reactions are shown in Figure 29. Each spectrum shown has the spectrum taken at t = 1.05 minutes subtracted in order to determine which peaks in the IR spectra corresponded to reactants from the pine-based cleaner and which peaks corresponded to products from reaction of the pine-based cleaner with ozone. As shown in this figure, there is loss of compounds in the OH stretching and carbonyl regions of the IR spectra. However, there is growth of a new product with peaks at 2860, 1595, and 1130 cm^{-1}. The growth of these peaks is consistent across all difference spectra obtained from these reactions, although the intensities of each peak differs based on the relative humidity and/or ozone concentration.

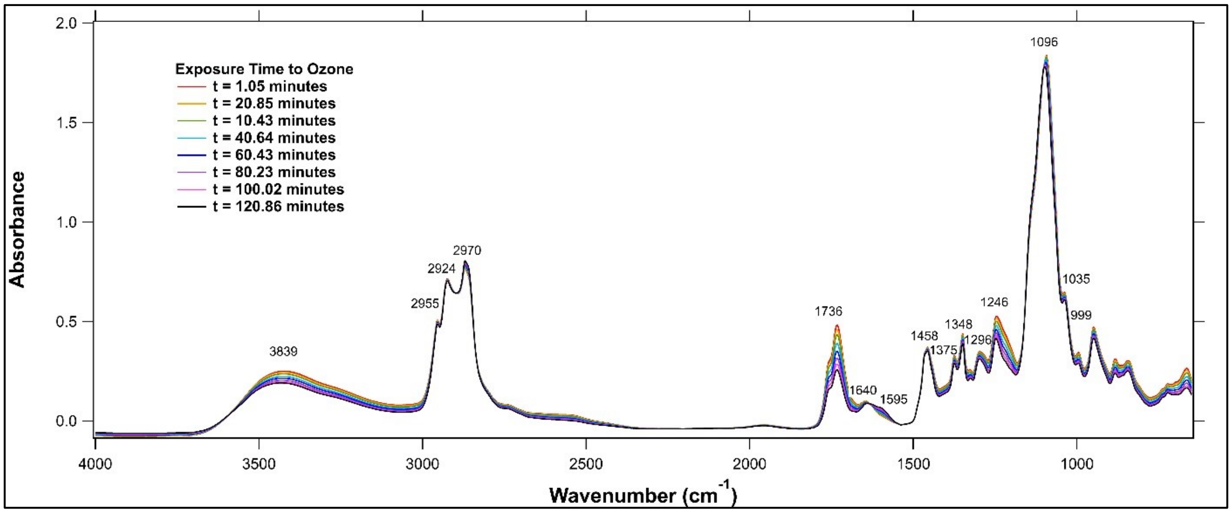

Figure 28: IR Spectra Obtained from ATR-IR Setup: Reactions of Pine-Based Cleaner and Ozone. Similar spectra were observed at varying relative humidities and ozone concentrations, but for this particular set of spectra were obtained at 46% RH and 92 ppb of ozone.

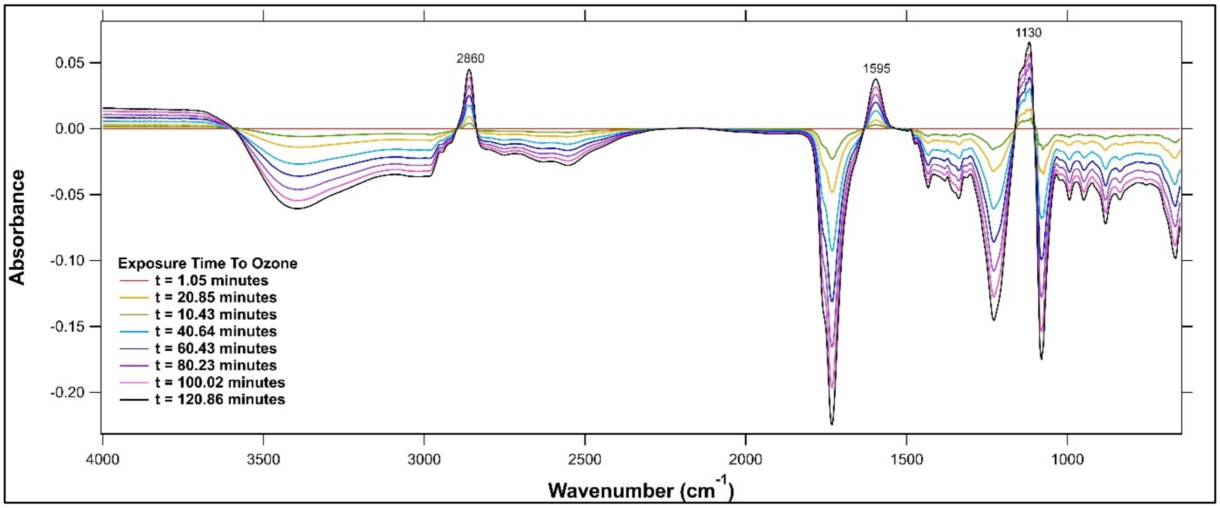

Figure 29: Difference IR Spectra Obtained from ATR-IR Setup: Reactions of Pine-Based Cleaner and Ozone. Similar spectra were observed at varying relative humidities and ozone concentrations, but for this particular set of spectra were obtained at 46% RH and 200 ppb of ozone.

Although the ATR-IR setup showed some growth of products from the reaction of the pine-based cleaner with ozone, the lemon-based cleaner showed less reactivity with ozone. Figure 30 shows several IR spectra over the course of a reaction of the lemon-based reaction with ozone. There is relatively no difference in peak intensity during ozone exposure to the pine-based cleaner. Even though no difference between spectra was observed, difference spectra were obtained and are shown in Figure 31. Each spectrum shown in this figure has the IR spectrum obtained at t = 1.05 minutes after exposure of the cleaner to ozone. Several peaks decay over the course of the reaction, including in the hydrocarbon region. However, several peaks also appear to grow in. One such peak is in the OH stretching region. Another peak also grows in in the carbonyl region (1714 cm^{-1}). An additional peak grows in at 1591 cm^{-1}. This peak has a similar wavenumber to a peak observed to grow in in the pine-based spectrum. Although these spectra were obtained at 62% relative humidity and 200 ppb of ozone, the spectra obtained for each reaction showed growth in the same positions and thus these sets of spectra are representative of many different relative humidities and concentrations. Several changes are also observed in the fingerprint region. This suggests that upon addition of ozone to the lemon-based cleaner in the thin film phase, new products are formed but in very low quantities.

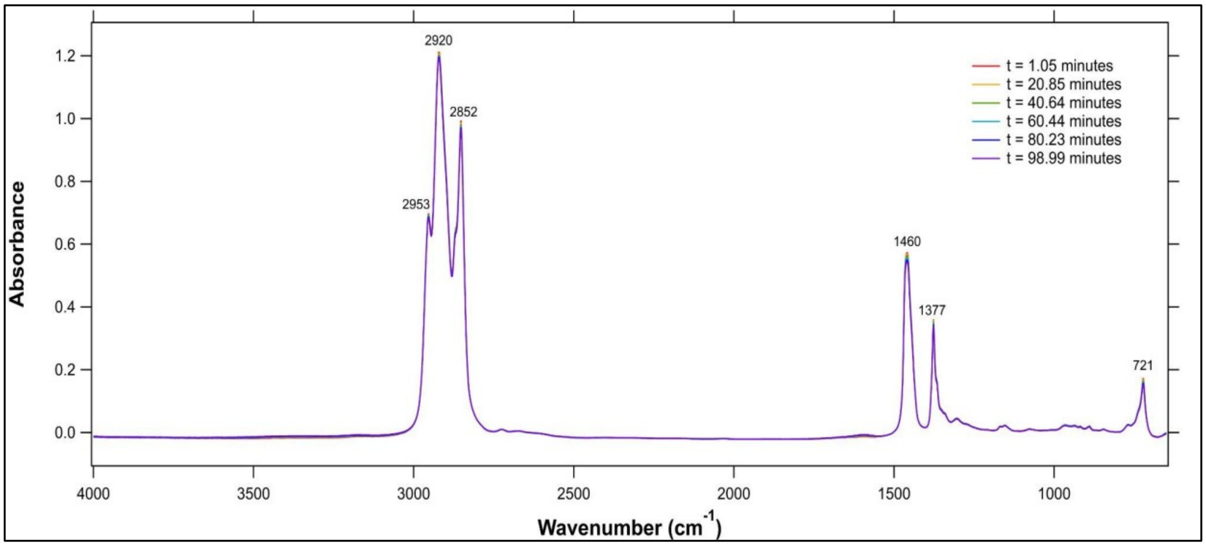

Figure 30: IR Spectra Obtained From Reaction of Lemon-Based Cleaner with Ozone Over 99 Minutes. RH = 77%, $[O_3]$ = 200 ppb.

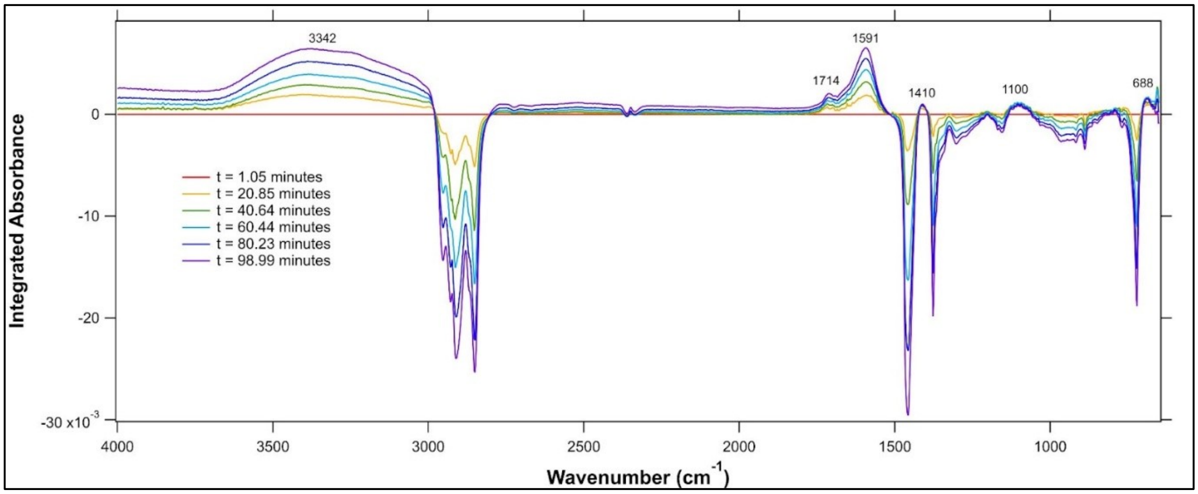

Figure 31: Difference Spectra Obtained From Reaction of Lemon-Based Cleaner with Ozone Over 99 Minutes. RH = 77%, $[O_3]$ = 200 ppb.

However, in comparing the ATR-IR results to the flow tube results, there is a marked difference in IR spectra. Figures 21 and 29 show difference IR spectra obtained from gaseous products leaving the flow reactor and organic compounds present in the thin film spectra, respectively. These IR spectra do not appear to show the same product. For instance, the IR spectra from ATR-IR show no carbonyls and different hydrocarbon growth. Additionally, the IR spectra from ATR-IR show a peak at 1600 cm^{-1} that is not present in the IR of flow tube products. This suggests that different products are formed from terpene ozonolysis in different phases. These results are somewhat unexpected; although previous work has shown that reaction rates can vary when the compound is in different phases, the identification of such different products using the same reactants is particularly intriguing and shows the diverse nature of the compounds present in the indoor environment formed from ozone and indoor cleaners.

3.4: Pine-Based Cleaner Kinetics

As shown in Figures 25 and 26, several peaks appeared to grow in upon exposure of the pine-based cleaner to ozone. Based on absorbance values observed in IR spectra, the rate at which these peaks grew in appeared to change based on relative humidity and/or ozone concentration tested. Since the peak position at 1600 cm^{-1} appeared to be the most consistent throughout the reactions conducted, this peak was integrated in each series of IR spectra over the course of each reaction. The pseudo rate constant (k) was obtained from Igor and plotted against the ozone concentration. Figure 32 shows the pseudo rate constants for the pine-based cleaner using at varying humidities but the same ozone concentration. As shown in this figure, there is no significant difference in reaction rate at different relative humidities. This process could not be repeated for the lemon-based cleaner due to insufficient product. Although this is consistent with the reactive uptake coefficients obtained in the laminar flow reactor, this result differs from previous research. Weschler claims that the presence of sorbed water causes increased reactivity on surfaces when the relative humidity increases (Weschler 2011). However, since the results in this study were consistent across many trials, it is likely that the compounds present in the cleaners used are unaffected in their reaction rates at different relative humidity levels.

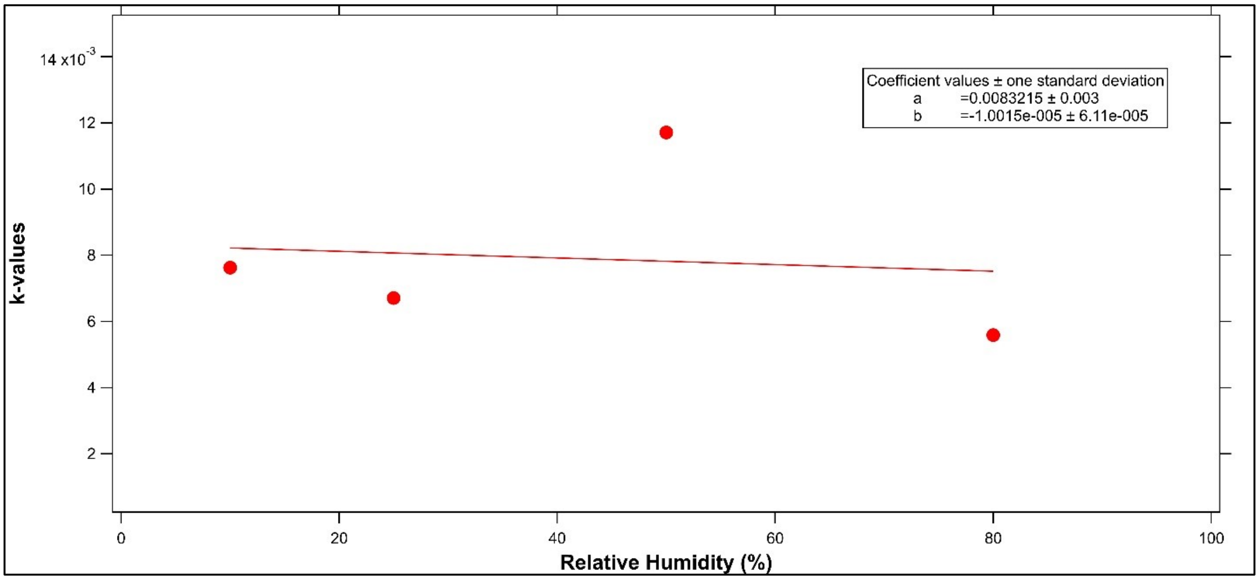

Figure 32: Pseudo Rate Constants at Varying Relative Humidity Levels. Although four different relative humidity levels are shown, all reactions were conducted with an $[O_3]$ = 200 ppb.

Conclusion

These results show that upon reaction of a pine-based terpene-containing cleaner with ozone, VOC products are observed. These compounds likely contain aldehydes, which have been shown to be particularly volatile and have negative effects on human health. Relative humidity also had no effect on the extent to which these reactions occurred in both methods. In contrast, the reaction of a lemon-based cleaner with ozone did not form new organic compounds, but rather increased the concentration of compounds already present in the cleaner. This result was unexpected, as the lemon and pine-based cleaner had similar chemical makeups. In particular, both contained limonene, a highly reactive terpene. Interestingly, the effective uptake coefficient of ozone did not change between the lemon and pine-based cleaners. Ultimately, both of these cleaners increased the presence of volatile organics in a chamber environment meant to mimic an indoor environment. The presence of VOCs from these methods suggests that the use of such products in an indoor environment can be dangerous for human health, especially in indoor settings in which the ozone concentration is high due to the corresponding outdoor environment and/or the use of appliances which produce ozone.

Although this study focused on ozone, there are many other pollutants prevalent in the indoor environment known to react with terpene-containing cleaners. Nitrogen oxides, in particular Nitrogen dioxide, is a pollutant that can react with such cleaners to produce VOCs and particulate matter, including SOAs. Future studies should seek to identify the products of these reactions to gain a more comprehensive understanding of the chemistry of indoor environments. Additionally, while this study used IR as the main method of product identification, other methods of chemical analysis can give further insight into the effects of cleaning products on indoor air quality. Particulate matter, especially fine and ultrafine PM, can form from reactions of indoor pollutants like ozone and Nitrogen oxide with terpene-based cleaners. Since these classes of particulate matter are extremely small and can enter the body very easily, it would be useful to identify the concentrations and components of such matter from reactions of cleaning products with indoor pollutants.

Bibliography

1. Fu, D.; Leng, C.; Kelley, J.; Zeng, G.; Zhang, Y.; Liu, Y. ATR-IR Study of Ozone Initiated Heterogeneous Oxidation of Squalene in an Indoor Environment. *Environ. Sci. Technol.* **2013**, 47, 10611-10618.
2. Weschler, C.J. Chemistry in indoor environments: 20 years of research. *Indoor Air*, **2011**, 21, 205-218.
3. Weschler, C.J.; Carslaw, N. Indoor Chemistry. Environ. Sci. Technol. **2018**, 52, 2419-2428.
4. Abbatt, J.P.D.; Wang, C. The atmospheric chemistry of indoor environments. *Environ. Sci.: Processes*, **2020**, 22, 25-48.
5. Nazaroff, W.W.; Weschler, C.J. Indoor ozone: Concentrations and influencing factors. *Indoor Air.* **2022**, 32, 1-21.
6. *World Health Organization.* https://www.who.int/news-room/fact-sheets/detail/ambient-(outdoor)-air-quality-andhealth#:~:text=The%20current%20WHO%20guideline%20value,effects%20of%20gaseous%20nitrogen%20dioxide (accessed 2022-11-01).
7. Wisthaler, A.; Tamas, G.; Wyon, D.P.; Strom-Tejsen, P.; Space, D.; Beauchamp, J.; Hansel, A; Mark, T.D.; Weschler, C.J. Products of Ozone-Initiated Chemistry in a Simulated Aircraft Environment. *Environ. Sci. Technol.* **2005**, 39, 4823-2832.
8. Salonen, H.; Salthammer, T.; Morawskia, L. Human exposure to ozone in school and office indoor environments. *Environ. Int.* **2018**, 119, 503-514.
9. Erickson, L.E.; Newmark, G.L.; Higgins, M.J.; Wang, Z. Nitrogen oxides and ozone in urban air: A review of 50 plus years of progress. *Environ. Prog. Sustainable Energy.* **2020**, 39, 1-9.

10. Zhong, L.; Lee, C.-S.; Haghihat, F. Indoor ozone and climate change. Sustain. Cities Soc. 2016, 28, 466-472.
11. Chen, X.; Hopke, P.K. A chamber study of secondary organic aerosol formation by limonene ozonolysis. *Indoor Air.* **2010**, 20, 320-328.
12. Tipayarom, A.; Tipayarom, D. Ozone Level Emitted from Photocopiers and its Exposure. *IPCBEE***. 2011**, 19, 42-47.
13. Weschler, C.J. Ozone in indoor environments: concentrations and chemistry. *Indoor Air***. 2000**, 10, 269-288.
14. Goldstein, A.H.; Nazaroff, W.W.; Weschler, C.J.; Williams, J. How Do Indoor Environments Affect Air Pollution Exposure? *Environ. Sci. Technol.* **2021**, 55, 100-108.
15. Milhelm, S.A.; Veriele, M.; Nicolas, M.; Thevenet, F. Does the ubiquitous use of essential oil-based products promote indoor air quality? A critical literature review. *Environ. Sci. Pollut. Res.* **2020,** 27, 14365-14411.
16. Liu, Y.; Misztal, P.K.; Arata, C.; Weschler, C.J.; Nazaroff, W.W.; Goldstein, A.H. Observing ozone chemistry in an occupied residence. *PNAS*. 2021, 6, 1-8
17. Donahue, N.M.; Tischuk, J.E.; Marquis, B.J.; Huff Hartz, K.E. Secondary organic aerosol from limona ketone: insights into terpene ozonolysis via synthesis of key intermediates. *Phys. Chem. Chem. Phys*. **2007**, 9, 2991-2998.
18. Singer, B.C.; Coleman, B.K.; Destaillats, H.; Hodgson, A.T.; Lunden, M.M.; Weschler, C.J.; Nazaroff, W.W. Indoor secondary pollutants from cleaning product and air freshener use in the presence of ozone. *Atmos. Environ.* **2006**, 40, 6696-6710.

19. Chiu, H.-H.; Chang, H.-M.; Lo, C.-C.; Chen, C.-Y.; Chiang, H.-L. Constituents of Volatile Organic Compounds of Evaporating Essential Oil. *Atmos. Environ.* **2009**, 43, 5743-5749.
20. Huang, H.-L.; Tsai, T.-J.; Hsu, N.-Y.; Lee, C.-C.; Wu, P.-C.; Su, H.-J. Effects of essential oils on the formation of formaldehyde and secondary organic aerosols in an aromatherapy environment. *Build Environ.* **2012**, 57, 120-125.
21. D'Ambro, E.L; Lee, B.H.; Liu, J.; Shilling, J.E.; Gaston, C.J.; Lopez-Hilfiker, F.D.; Schobesberger, S.; Zaveri, R.A.; Mohr, C.; Lutz, A.; Zhang, Z.; Gold, A.; Surratt, J.D.; Rivera-Rios, J.C.; Keutsch, F.N.; Thornton, J.A. Molecular composition and volatility of isoprene photochemical oxidation secondary organic aerosol under low- and high-NO_x conditions. *Atmos. Chem. Phys***.** **2017**, 17, 159-174.
22. Chen, J.; Moller, K.H.; Wennberg, P.O.; Kjaegaard, H.G. Unimolecular Reactions Following Indoor and Outdoor Limonene Ozonolysis. *J. Phys. Chem*. **2021**, 125, 669-680.
23. Jaoui, M.; Corse, E.; Kleindienst, T.E.; Offenberg, J.H.; Lewandowski, M.; Edney, E.O. Analysis of Secondary Organic Aerosol Compounds from the Photooxidation of d-Limonene in the Presence of NO_x and their Detection in Ambient $PM_{2.5}$. *Environ. Sci. Technol.* **2006**, 40, 3819-3828.
24. Fiedler, N.; Laumach, R.; Kelly-McNeil, K.; Lioy, P.; Fan, Z.-H.; Zhang, J.; Ottenweller, J.; Ohman-Strickland, P.; Kipen, H. Health Effects of a Mixture of Indoor Air Volatile Organics, Their Ozone Oxidation Products, and Stress. *Environ. Health Perspec.* **2005**, 113, 1542-1548.

25. Tamas, G.; Weschler, C.J.; Toftum, J.; Fanger, P.O. Influence of Ozone-Limonene Reactions on Perceived Air Quality. *Indoor Air*. **2006**, 16, 168-178.
26. Markowicz, P.; Larsson, L. Influence of relative humidity on VOC concentrations in indoor air. *Environ. Sci. Pollut. Res.* **2015**, 25, 5772-5779.
27. Su, H.-Y.; Chao, C.-J.; Chang, H.-Y.; Wu, P.-C. The effects of evaporating essential oils on indoor air quality. Atmos. Environ. 2007, 41, 1230-1236.
28. Wolkoff, P.; Kjægaard, S.K. The dichotomy of relative humidity on indoor air quality. *Environ. Int.* **2007**, 33, 850-857.
29. Coates Fuentes, Z.L.; Kucinski, T.M; Hinrichs, R.Z. Ozone Decomposition on Kaolinite as a Function of Monoterpene Exposure and Relative Humidity. *ACS Earth Space Chem.* **2018**, 2, 21-30.
30. Ausili, A.; Sanchez, M.; Gomez-Fernandez, J.C. Attenuated total reflectance infrared spectroscopy: A powerful method for the simultaneous study of structure and spatial orientation of lipids and membrane proteins. *BSI*. **2015**, 4, 159-170.
31. Fu, D.; Leng, C.; Kelley, J.; Zeng, G.; Zhang, Y.; Liu, Y. ATR-IR Study of Ozone Initiated Heterogeneous Oxidation of Squalene in an Indoor Environment. *Environ. Sci. Technol.* **2013**, 47, 10611-10618.
32. Destaillats, H.; Lunden, M.M.; Singer, B.C.; Coleman, B.K.; Hodgson, A.T.; Weschler, C.J.; Nazaroff, W.W. Indoor Secondary Pollutants from Household Product Emissions in the Presence of Ozone: A Bench-Scale Chamber Study. *Environ. Sci. Technol.* **2006**, 40, 4421-4428.
33. Wells, J.R. Use of denuder/filter apparatus to investigate terpene ozonolysis. *J. Environ. Monit.* **2012**, 14, 1044-1054.

34. National Institute of Standards and Technology Chemistry WebBook. https://webbook.nist.gov/cgi/inchi?ID=C1482015&Mask=80. (accessed 2022-11-01).

35. National Institute of Standards and Technology Chemistry WebBook. https://webbook.nist.gov/cgi/cbook.cgi?ID=50-00-0. (accessed 2022-11-01).

36. Ramasamy, S.; Nakayama, T.; Morino, Y.; Imamura, T.; Kajii, Y.; Enami, S.; Sato, K. Nitrate radical, ozone and hydroxyl initiated aging of limonene secondary aerosol. *Atmos. Environ.* **2021**, 1-10.

37. Piletic, I.R.; Kleindienst, T.E. Rates and Yields of Unimolecular Reactions Producing Highly Ozidized Peroxy Radicals in the OH-Induced Autoxidation of α-Pinene, β-Pinene, and Limonene. *J. Phys. Chem*. **2022**, 126, 88-100.

38. Chen, X.; Hopke, P.K.; Carter, W.P. Secondary Organic Aerosol from Ozonolysis of Biogenic Volatile Organic Compounds: Chamber Studies of Particle and Reactive Oxygen Species Formation. *Environ. Sci. Technol*. **2017**, 276-282.